

Lawrence Berkeley National Laboratory

Recent Work

Title

CHEMICAL VAPOR DEPOSITION OF GaAs_{1-x}P_x REACTOR DESIGN AND GROWTH KINETICS

Permalink

<https://escholarship.org/uc/item/60r3247r>

Author

Shaikh, Saleem A.

Publication Date

1972-09-01

RECEIVED
LAWRENCE
BERKELEY LABORATORY

LBL-1149

LIBRARY AND
DOCUMENTS SECTION

CHEMICAL VAPOR DEPOSITION OF $\text{GaAs}_{1-x}\text{P}_x$ REACTOR
DESIGN AND GROWTH KINETICS

Saleem A. Shaikh
(M.S. Thesis)

September 1972

AEC Contract No. W-7405-eng-48

For Reference

Not to be taken from this room



LBL-1149

DISCLAIMER

This document was prepared as an account of work sponsored by the United States Government. While this document is believed to contain correct information, neither the United States Government nor any agency thereof, nor the Regents of the University of California, nor any of their employees, makes any warranty, express or implied, or assumes any legal responsibility for the accuracy, completeness, or usefulness of any information, apparatus, product, or process disclosed, or represents that its use would not infringe privately owned rights. Reference herein to any specific commercial product, process, or service by its trade name, trademark, manufacturer, or otherwise, does not necessarily constitute or imply its endorsement, recommendation, or favoring by the United States Government or any agency thereof, or the Regents of the University of California. The views and opinions of authors expressed herein do not necessarily state or reflect those of the United States Government or any agency thereof or the Regents of the University of California.

CHEMICAL VAPOR DEPOSITION OF $\text{GaAs}_{1-x}\text{P}_x$
REACTOR DESIGN AND GROWTH KINETICS

Contents

Abstract	v
I. General Introduction	1
Bibliography	4
II. Reactor Design	5
A. Introduction	
B. Survey of Research Reactors	6
C. Design Problems	9
D. Commercial Applications	15
Bibliography	17
Figure Captions	19
Figures	20
III. Thermodynamics of Phase Equilibria for Chemical Vapor Deposition of $\text{GaAs}_{1-x}\text{P}_x$	22
A. Introduction	
B. Reaction Equilibria in the Ga-As-P-H-Cl System	23
C. Gallium Saturation Equilibria	30
D. Reaction Zone Equilibria	33
E. Deposition Zone Equilibria	38
F. Results and Discussion	43
Bibliography	48
Figure Captions	50
Figures	51

IV. Deposition Kinetics	64
A. Introduction	
B. Theory of Diffusion Limited Kinetics	65
C. Boundary Layer Models	67
D. Calculation of Deposition Rates	70
E. Results and Discussion	72
Bibliography	74
Figure Captions	75
Figures	76
V. Experimental Study of $\text{GaAs}_{1-x}\text{P}_x$ Chemical Vapor Deposition .	80
A. Introduction	
B. Reactor and Gas Flow System	
C. Operation of the System	82
D. Results and Discussion	83
Bibliography	88
Figure Captions	89
Figures	90
VI. Conclusions	95
Acknowledgements	98
Appendices	99

CHEMICAL VAPOR DEPOSITION OF GaAs_{1-x}P_x
REACTOR DESIGN AND GROWTH KINETICS

Saleem A. Shaikh

Inorganic Materials Research Division, Lawrence Berkeley Laboratory
and Department of Chemical Engineering; University of California
Berkeley, California

ABSTRACT

The chemical vapor deposition of GaAs_{1-x}P_x from Ga(l), PH₃, AsH₃, HCl and H₂ source chemicals is studied, both theoretically and experimentally in a research reactor, in terms of reactor design, thermodynamics of phase equilibria and diffusion limited deposition kinetics.

Reaction processes for the chemical vapor deposition of GaAs_{1-x}P_x are reviewed, and basic principles in the design of research and commercial reactors are discussed with respect to optimum performance, efficiency and production yield. Thermodynamics of phase equilibria in the Ga-As-P-Cl-H system are examined for each zone of the reactor, and analytical procedures developed for calculating equilibria in terms of reduced variables. Deposition rates and efficiencies are estimated assuming diffusion controlled kinetics and boundary layer models.

Deposition rates and alloy composition were studied as a function of reactor conditions in an experimental reactor utilizing design principles. Experimentally obtained alloy compositions agree well with the predicted ones but the experimental growth rates are too low.

I. GENERAL INTRODUCTION

The production of $GaAs_{1-x}P_x$ by chemical vapor deposition (CVD) has become very important in the recent years.¹ The chief use of these compounds is in the electronic industry where the compositions of commercial applications are $x = 0.6$ and 0.19 . The first composition is required in the manufacture of light emitting diodes² and second in solid state hetero-junction lasers.³ The expansion of commercial applications of $GaAs_{1-x}P_x$ crystals and epitaxial thin films has been so great in recent years that the supply has become the limiting factor.⁴ The main reason why this compound is preferred over other classes of electronic materials lies in its relatively easy and low cost of synthesis and epitaxial growth on a supporting substrate. The industrial applications of epitaxial III-V compound alloys has established a need for better designs of chemical vapor deposition apparatus for increased efficiency and uniformity of product. This requires a better understanding of the overall process. The purpose of this work is to provide a comprehensive study of the growth process, thermodynamics of the system and reactor design.

Although many experimental studies of III-V alloy growth by chemical vapor deposition have been reported, only recently has this process been the subject of theoretical study. For example the growth process for GaAs has been studied in great detail following the inspiring work of Newman⁵ in 1961. Reactors with varying designs were employed in these experimental studies. However the theoretical aspects of the growth process were not studied until 1966 when Hurle and Mullin⁶ outlined a general approach to the calculation of phase equilibria in the Ga-As-H-Cl system on the basis of which the feasibility of the reaction could be assessed from thermo-

dynamic data. Seki^{7,8} used a similar approach to solve the system Ga-P-H-Cl. Later studies extended these calculations to phase equilibria involving GaAs_{1-x}P_x.^{9,10} Kirwan¹¹ and others have aided these calculations by measuring the equilibrium constants for reactions which can take place in the Ga-As-P-Cl-H system.

The diffusion controlled growth process has been studied in depth by Goettler¹² whose approach coupled the thermodynamic constraint with diffusion processes in the deposition zone to obtain the growth rate for the process.

Chemical vapor deposition of GaAs_{1-x}P_x alloys is achieved by processes analogous to that of GaAs and it is anticipated that future work will concentrate on analyzing more and more complex systems after sufficient experimental work has been reported.

The first study of GaAs_{1-x}P_x growth was reported by Finch and Mehal¹³ in 1964 and since then many experimentalists have grown this alloy in all compositions. However the thermodynamics of the system were only recently analyzed by Manabe¹⁴ and by Bleicher.¹⁵ These two workers, however, neglected the growth process itself and concentrated more on phase equilibria in the reactor. Further analysis of chemical vapor deposition is essential if the optimum efficiency and product uniformity is to be achieved commercially, where the primary interest is on lower cost and higher yield.

The present study examines the overall chemical vapor deposition process in three parts: In the first part, the reactor design is discussed after a survey of various reactors used in research and industry. An effort is made to analyze the problem from the standpoint of efficiency and production yield. The second part consists of a thermodynamic study of phase equilibria. A simplified approach is used to correctly predict

the various equilibrium properties of the system. This part is also aimed at predicting the driving forces available for the deposition process. In the third part, deposition kinetics are studied based on a model for diffusion controlled growth. Experimental data are obtained from an experimental reactor operated at different degrees of departure from equilibrium. The experimental and theoretically predicted deposition rates and product composition are compared.

These three parts give a comprehensive picture of the chemical vapor deposition of $\text{GaAs}_{1-x}\text{P}_x$ through fundamental analysis of reactor design, phase equilibria and diffusion controlled growth. The results of the study should provide techniques for better reactor design, better control and greater uniformity of the deposition of the alloys as well as of the pure compounds.

BIBLIOGRAPHY

1. R. A. Ruherwein, "Manufacturing Methods for Growing GaAs, GaP Single Crystal Alloys" Contract no: AFML-TR-68-319, Monsanto Co., St. Louis, Mo., October 1968.
2. R. Saul, J. Appl. Phys. 40, 3273 (1970).
3. M. G. Craford and W. O. Grovesand, J. Electrochem. Soc. 118, 355 (1971).
4. R. S. Polzer and W. C. Benzing, Applied Materials Technology Report, Santa Clara, California (1972).
5. R. L. Newman, J. Electrochem. Soc. 108, 1127 (1961).
6. D. T. J. Hurle and J. B. Mullin, J. Phys. Chem. Solids, Supplement 1, pp. 241-8 (1966).
7. H. Seki and H. Araki, Japan J. Appl. Phys. 6, 1414 (1967).
8. H. Seki, et al., Japan J. Appl. Phys. 7, 1324 (1968).
9. H. Seki and H. Eguchi, Japan J. Appl. Phys. 10, 39 (1971).
10. I. Amron, J. Electrochem. Soc. 118, 1026 (1971).
11. D. J. Kirwan, J. Electrochem. Soc. 117, 1572 (1970).
12. L. A. Goettler, "Diffusion and Surface Kinetics in the Epitaxial Vapor Deposition of GaAs," AIChE 67th National Meeting, Feb. 1970.
13. W. F. Finch and E. W. Mehal, J. Electrochem. Soc. 111, 814 (1969).
14. T. Manabe, "Thermodynamic Analysis of the Ga-As-P-Cl-H System for Vapor Growth of GaAs_{1-x}P_x" Third International Conference on CVD, April 1972, pp. 25-36.
15. M. Bleicher, J. Electrochem. Soc. 119, 613 (1972).

II. REACTOR DESIGN

A. Introduction

Processes for the growth of epitaxial layers of GaAs, GaP and GaAs_{1-x}P_x by chemical vapor deposition (CVD) have been known since the early 1960's, and are essentially the same for either of the two pure compounds or their alloy, but different chemical reactions are involved. Many of these processes utilize chemical transport reactions as developed by Schaeffer,¹ but many of the consequences apply to chemical vapor deposition as well. When the desired product is also the source of transported components the temperature of the deposition zone must be higher than that of the source for transport reactions with a positive entropy change. The temperature of the source and deposition zones is usually lower than that of the connecting zone to prevent undesired deposition. For high crystallographic perfection of the deposit, the driving force as measured by the temperature difference between the source and substrate must not be too large or an uneven deposit is produced. If the driving force is too small the growth is slow, and therefore a temperature difference of 15-30°C is most often used.

A basic transport process consists of reacting liquid gallium (source) with an oxidizing agent to form a volatile compound of gallium which is mixed with a volatile form of arsenic and/or phosphorous and transported to a zone where the gas phase is supersaturated with respect to the solid. Growth takes place at surfaces where the gases react to condense the III-V compound. Because the number of volatile compounds is large, as is the number of possible ways of reacting them, many reactor designs have been developed to explore this process.

Owing to the high costs of reactants for the chemical vapor deposition of $\text{GaAs}_{1-x}\text{P}_x$ and for other III-V compounds--the deposition reaction must be carried out in the diffusion-controlled regime. Hot wall reactors are used for III-V compound deposition in order to prevent condensation of GaCl which is volatile only at high temperatures. This choice is contrary to reactors used for silicon where the silane transport species are relatively more volatile at lower temperatures and cold wall, heated substrate conditions can be used.

Essentially all of the GaAs, GaP or $\text{GaAs}_{1-x}\text{P}_x$ reactors are open flow types (constant pressure). A sealed tube reactor (constant-volume) is not usual due to the large number of reactants involved and difficulty in controlling the growth. The open flow reactors are semi-continuous batch type in which a number of substrates can be placed for epitaxial growth with an infinite choice of conditions.

B. Survey of Research Reactors

Schematic diagrams of the various reactors which have been proposed for growing GaAs, GaP and $\text{GaAs}_{1-x}\text{P}_x$ are shown in Fig. 1. Early reactors used both arsenic and gallium in the solid form as starting materials but later AsH_3 or AsCl_3 replaced solid arsenic as a transport species. Attempts were made to use other oxidizing agents besides the halides, and principally chlorides. H_2O was used for oxidizing gallium to Ga_2O in a process called the wet-hydrogen process.²

Figure 1a shows the flow-through reactor used by Newman³ and by Minden⁴ for GaAs in 1961. They simply chlorinated arsenic and gallium and deposited the solids on a GaAs substrate. The reactor was a horizontal type with three temperature regions. Goldsmith⁵ modified this

reactor and placed the substrate in the middle of the arsenic and gallium sources, the substrates being placed in a side tube. This design used GaCl₃ as the starting material. The reason why this study used such a low-temperature for the Ga(l) is not apparent. Possibly the GaCl₃ reacted with Ga(l) to form the GaCl transport species. However, according to the data published by Kirwan⁶ at a much later date, GaCl₃ is the most stable chloride of gallium at lower temperatures, and only at temperatures of 600°C does GaCl become important. Amick⁷ and Michelitsch⁸ used HCl instead of GaCl₃ in essentially the same process as used by Goldsmith, and the reactor temperatures were also the same. In 1965, Effer⁹ modified the Newman-Minden version of the reactor by using AsCl₃ as starting material for arsenic instead of pure arsenic (Fig. 1d).

The advantages of introducing a gaseous species at the input instead of a solid as a source of arsenic are so great in terms of ease and controllability that few subsequent reactor studies have used arsenic in the solid form. In the liquid form AsCl₃ is safer than other arsenic sources, and also the rate of vaporization can be controlled more easily than can solid arsenic. Once the advantages of using a gaseous arsenic source were realized other sources besides AsCl₃ were exploited. AsCl₃ still had the disadvantage that because it is a liquid, hydrogen has to be bubbled through it with great care to prevent variations in AsCl₃ vapor pressure. However, AsH₃ is a gas at standard temperature and pressure and can be introduced at precise flow rates. Therefore control of the growth process is much easier and precise. Teitjen¹² first used AsH₃ as a source of arsenic in 1966 and reacted gallium with HCl to form

GaCl and GaCl₃. Shaw¹³ in 1968 employed As (solid) again in 1970 but subsequently modified his reactor to the form used earlier by Tietjen and others.

The reactors for GaP are essentially the same as those for the deposition of GaAs. However, because GaP was explored much later as a potential electronic device material, the reactor studies placed more emphasis on deposition uniformity and its dependence on the orientation of the substrate holder. The work of Luther¹⁴ is a very good example and the design of the substrate holder is treated in great detail. He showed that if liquid N₂ is passed under the substrate to cool it, the growth is faster and planar because the gradient in temperature on the growing surface does not allow constitutional supercooling which causes the planar growing surface to become unstable with respect to protrusions. In his reactor the substrate is placed at an angle to the gas flow direction as shown in Fig. 11. Goettler¹⁷ designed a vertical reactor in 1970 in which the substrate is again at an angle rather than being parallel to the flow direction. In silicon reactors and later studies of GaAs_{1-x}P_x deposition the substrates are usually placed at an angle to, or normal to the flow direction rather than parallel to the flow direction as used by all earlier studies. The reactants for GaAs_{1-x}P_x and the reactor itself are essentially the same as for GaAs and GaP. This is apparent from the studies made by Ban,¹⁸ Manabe,¹⁹ and Bleicher.²⁰

The substrate placement in the reactor is an important aspect of the reactor design itself since the velocity distribution for gases flowing over the substrate controls the uniformity of the growth rate, and this

is influenced by the direction of flow. The flow properties of the gases and the geometry of the system also affect the growth rate uniformity.

C. Design Problems

There are numerous problems associated with the optimal design of CVD reactors. Basically the reactor must have a gallium saturation zone where a volatile compound of gallium is generated, a deposition zone containing the substrates where deposition takes place and a central zone where the various gaseous species mix and react to produce a high temperature equilibrium between As_4 , P_4 , etc. We will call these zones the saturation deposition and reaction zones respectively. It has been found that gallium metal is the best starting material for gallium and is available in 99.9999% purity but for arsenic and phosphorous the chemical purity is not as high. Gaseous forms of arsenic and phosphorous are preferred over liquid forms or solid arsenic and phosphorous. Gaseous forms are the halides at high temperature, e.g. the chloride or hydride.

Other variables in reactor design which can be raised are:

1. A horizontal versus a vertical reactor orientation,
2. the source compounds for arsenic and phosphorous,
3. the structure of the gallium saturator,
4. the flow geometry and its control for uniform deposition
5. the choice of substrate in the reactor and
6. the choice of containment and support materials within the reactor.

In order to assess these variables, several will be examined in greater detail in the following sections.

1. Horizontal and Vertical Reactors

Both horizontal and vertical reactors have been used in GaAs, GaP, and GaAs_{1-x}P_x deposition processes. The vertical reactor was developed by Goettler⁴ in 1970. It has advantages over the horizontal type. The gases used in the growth process using group V halides and HCl/H₂ over liquid gallium are carried by hydrogen which is a very light gas. The typical flow regime in the reactor is laminar which means that mixing is slow. The gases which take part in the deposition equilibrium i.e., GaCl, GaCl₃, HCl, As₄, As₂, P₄ and P₂ in the Ga-As-P-H-Cl system are much heavier. Therefore, in a gravitational field, if the reactor is of a horizontal type, the reactants will tend to concentrate on the bottom wall which will give rise to an uneven distribution and poor efficiency of the reaction. In the vertical type reactor, the heavy gases can be more easily directed toward the substrates. Of course, turbulent mixing of transport gases can improve gas uniformity of either type.

Another disadvantage of horizontal flow reactor is that the gases will tend to create backflow due to any difference in temperature between the top wall and substrate whereas in the vertical reactor, this effect is negligible.

Therefore it is suggested that a vertical reactor is better than a horizontal type for growth of GaAs_{1-x}P_x.

2. Source Compounds for Arsenic and Phosphorous

The two preferred source compounds for arsenic (or phosphorous) are AsCl₃ (PCl₃) and AsH₃ (PH₃). As was seen in the survey of previous reactors the chloride normally is passed over gallium to obtain GaCl and GaCl₃. The combined gases are then transported to the substrate for deposition.

The reaction of the chloride on gallium surfaces is not controllable precisely, because GaAs or GaP is formed on the surface of the liquid gallium. The rate of formation of surface coating is unknown and a good control of growth is not possible. On the other hand the hydride decomposes to arsenic and phosphorous and reacts with gallium only on the surface of the substrate. The decomposition of the hydride is almost complete (see Chapter III) at high temperature ($\sim 900^\circ\text{C}$). So the arsenic or phosphorous in the elemental form reacts with the major species, GaCl, on the surface of the substrate.

Another reason for preference for the hydride over the chloride is that the chloride is in liquid form at standard temperature and pressure, and must be volatilized to be introduced into the reactor. For the hydride no such problem exists because it is already in gaseous form and can be easily metered through a metering valve and flowmeter.

Therefore, the hydrides (AsH_3 and PH_3) are preferred as starting materials over other types. This choice is supported by the increased purity and availability of arsine and phosphine for electronics materials applications.

3. Gallium Saturator

In all of the recent reactor designs, HCl has been used in the chlorination of gallium. This is partially due to the fact that HCl is found in the gaseous form. Another good reason is that it reacts almost completely with the gallium to form GaCl instead of GaCl_3 . According to recent studies GaCl is the reacting species which is mechanically responsible for growing $\text{GaAs}_{1-x}\text{P}_x$. A previously held contention that GaCl_3 is the major reacting species was shown by Kirwan⁶ and others,

to be incorrect. The main problem in design of the saturator is to assure good contact of HCl with gallium to achieve equilibrium in the saturator. Although the problem involves simultaneous mass transfer and chemical reaction, it has not been studied in detail by earlier workers. Ban¹⁸ shows that about 80% of HCl is converted to GaCl at 850°C by HCl gas flowing over an open gallium boat. Goettler achieved essentially complete equilibrium in a toroidal saturator. Thermodynamic equilibria suggests that 99.9% HCl should be converted to GaCl at 850°C.

In order to approach equilibrium at the gallium contactor (boat) the HCl should have sufficient contact time to equilibrate. The gallium contactor can be of three types:

1. HCl/H₂ gas flowing over the liquid gallium in laminar flow,
2. Gas impinging on liquid gallium in turbulent flow,
3. Gas bubbling through liquid gallium.

The third process is the most efficient means of mass transfer of the three types.

For a gas bubbler, the gas bubbles should be reduced to small sizes by passing them through a jet or dispenser to increase the surface area for reaction and hence the conversion efficiently. The reactor designed by Goettler¹⁷ uses such a liquid gallium bubbler.

4. Mixing of Gases

Before the gases reach the substrate for deposition, they should be well mixed and given a uniform velocity profile. Therefore a mixing region is necessary after the gallium saturator zone where arsenic and phosphorous in the elemental form can mix with the effluent stream from the gallium boat. In this region nearly complete decomposition of

As H_3 and PH_3 also takes place. Therefore the gases should have a sufficient residence time here. These objectives may be achieved by increasing turbulence in a mixing region and by restricting the flow to the deposition zone. Mixing can be done by providing a nozzle or orifice in the reactor between the gallium saturation and deposition zone. To make the flow of gases over the substrate as uniform as possible, however, the gases should be allowed to pass through a sieve or allowed to flow at low Reynolds number through a calming length in the reactor.

5. Substrate Positioning

For a uniform deposition thickness over a substrate which is required for electronic grade materials, the gases should have a uniform composition and they should contact the substrate with uniform velocities. But due to the diffusion controlled kinetics at high temperatures a boundary layer is formed over the substrate by the incoming gases. The thickness of the boundary layer may vary from one part to another; which in turn affects the deposition rate uniformity. This problem can be decreased by a proper positioning of the substrate. For flow parallel to the flow direction of the gases, the laminar boundary layer will increase in thickness from the point where gases first reach the substrate throughout the length of the substrate. Temperature variations along the substrate will also affect the rate of reaction. For flow normal to the substrate, the boundary layer thickness will decrease towards the edges of the substrate, and the nonuniformity of the layer will cause a nonuniform growth. When flow is at an angle to the substrate, the boundary layer will have a structure between the two above cases. This positioning has been used in many recent studies.

In some research reactors and in commercial reactors, the substrate is rotated and because of the slight turbulence caused by the rotation, the boundary layer becomes more uniform. A complete solution of this problem is not yet found. The best arrangement seems to be the rotation of the substrate at an angle to the flow of the gases.

D. Commercial Applications

Development of commercial reactors for CVD of $\text{GaAs}_{1-x}\text{P}_x$ has been reported by the Monsanto Research Corporation²¹ and Applied Materials Technology.²²

Monsanto Research Corporation carried out an extensive study of the manufacturing methods for epitaxial growth of GaAs and GaP in 1968, including the study of various reactor designs. They used both horizontal and vertical reactors employing PH_3 , AsH_3 , HCl and $\text{Ga}(\ell)$ in this process. Both turbulent and laminar flows of reactant gases across the substrate were explored. Their study showed that a vertical reactor with laminar gas flow is best suited for the growth of GaAs or GaP by chemical vapor deposition.

The Monsanto study included the design of gallium-HCl reaction vessels and substrate holders, employing various designs for flowing HCl-H₂ gases over liquid gallium, gases impinging on gallium through a jet, or bubbling through gallium. They found that a bubbler is best suited for maximum efficiencies of conversion but a cover over the gallium container is required in order to keep gallium from spilling out of the container. Their design of the gallium saturator is shown in Fig. 2(a). Also this study concluded that a rotating pyramid substrate holder (5-40 rpm) produces the best conditions for a uniform deposition. The gases flow oblique to the substrate and the boundary layer is compressed, becoming more uniform. The rotation speed of the substrate holder can be varied according to the deposition desired. The schematic of the pyramidal substrate holder is also shown in Fig. 2(a). The pyramid has eight sides and can hold up to eight substrates.

Additional HCl gas can be introduced to prevent deposition on reactor walls. Extensive data have also been published for diverse conditions of growth.

The $\text{GaAs}_{1-x}\text{P}_x$ reactor manufactured by Applied Materials Technology is shown in Fig. 2(b). This reactor developed in 1971-72 is also a hot wall reactor but fits within a bell jar. Its essential features are:

1. Vertical flow of the gases downward across obliquely held substrates.
2. A GaCl generator in which HCl bubbles through liquid gallium contained in a cylindrical boat.
3. Substrate holder of a truncated pyramidal shape which can be rotated at any desired speed, and able to hold up to eight substrates. (The holder is coated with silicon carbide)
4. Uses AsH_3 and PH_3 as starting materials for arsenic and phosphorous.

A very good feature of this reactor is that purge gases enter the bell jar at critical points near the reactor walls to avoid any deposition there and to prevent contamination when the bell jar is opened.

The only seal that is broken between the runs is between the bell jar and its base plate, keeping leakage to a minimum and increasing the ease of handling of the reactor.

BIBLIOGRAPHY

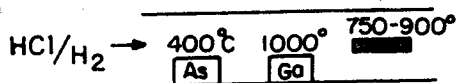
1. H. Schaffer, Chemical Transport Reaction, (Academic Press, N. Y. 1964).
2. L. D'yakonov, *Isv. Akad. Nauk, SSSR, Neorg. Mat.* 1, 1892 (1965).
3. R. L. Newman, *J. Electrochem. Soc.* 108, 1127 (1961).
4. S. W. Ing, *J. Electrochem. Soc.* 109, 995 (1962).
5. N. Goldsmith, *RCA Review* 29, 546 (1963).
6. D. J. Kirwan, *J. Electrochem. Soc.* 117, 1572 (1970).
7. J. A. Amick, *RCA Review* 29, 555 (1963).
8. M. Michelitsch, *J. Electrochem. Soc.* 112, 747 (1965).
9. D. Effer, *J. Electrochem. Soc.* 112, 747 (1965).
10. K. L. Lawly, *J. Electrochem. Soc.* 113, 240 (1966).
11. M. Rubenstein, *J. Electrochem. Soc.* 113, 365 (1966).
12. J. J. Teitjen, *J. Electrochem. Soc.* 113, 724 (1966).
13. D. W. Shaw, *J. Electrochem. Soc.* 115, 777 (1968).
14. L. C. Luther, *Met. Trans.* 1, 593 (1970).
15. C. M. Ringel, *J. Electrochem. Soc.* 118, 609 (1971).
16. W. F. Finchland and E. W. Mehal, *J. Electrochem. Soc.* 111, 814 (1964).
17. L. A. Goettler, "Diffusion and Surface Kinetics in the Epitaxial Vapor Deposition of G As", AIChE 67th National Meeting, Feb. 1970.
18. V. S. Ban, *J. Electrochem. Soc.* 118, 1473 (1971).
19. T. Manabe, "Thermodynamic Analysis of the Ga-As-P-Cl-H System for Vapor Growth of $\text{GaAs}_{1-x}\text{P}_x$ ", Third International Conference on CVD, April 1972, pp. 25-36.
20. M. Bleicher, *J. Electrochem. Soc.* 119, 613 (1972).

21. R. A. Ruherwein, "Manufacturing Methods for Growing GaAs, GaP Single Crystal Alloys", Contract no: AFML-TR-68-319, Monsanto Co., St. Louis, Mo., October 1968.
22. R. S. Pelser and W. C. Benzing, Report by Applied Materials Technology, Inc., Santa Clara, Calif. (1972).

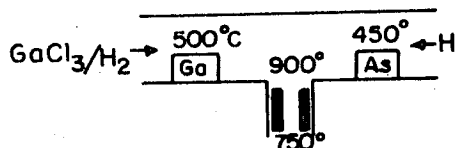
Figure Captions

- Fig. 1. Research reactors for chemical vapor deposition of GaAs, GaP and $\text{GaAs}_{1-x}\text{P}_x$.
- Fig. 2. Industrial reactors for epitaxial deposition of $\text{GaAs}_{1-x}\text{P}_x$.
- a. Monsanto reactor b. AMT reactor

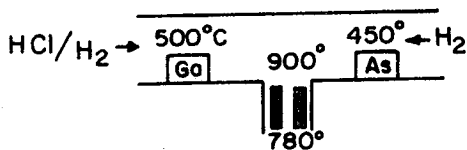
a. Newman⁽³⁾ and Minden⁽⁴⁾



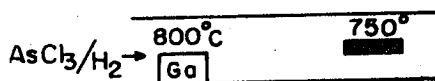
b. Goldsmith⁽⁵⁾



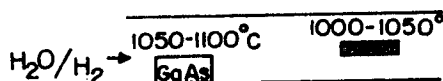
c. Amick⁽⁷⁾ and Michtelsch⁽⁸⁾



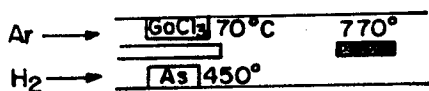
d. Effer⁽⁹⁾



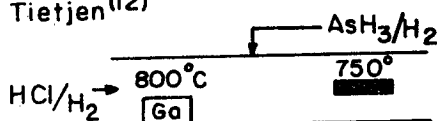
e. Lawly⁽¹⁰⁾



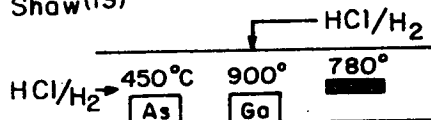
f. Rubenstein⁽¹¹⁾



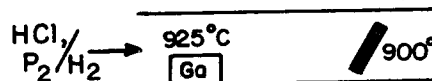
g. Tietjen⁽¹²⁾



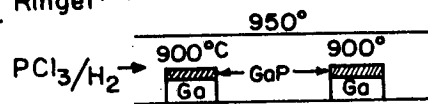
h. Shaw⁽¹³⁾



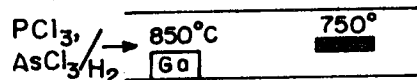
i. Luther⁽¹⁴⁾



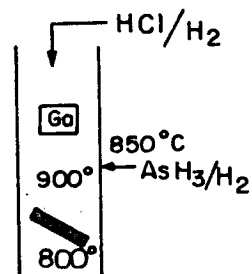
j. Ringel⁽¹⁵⁾



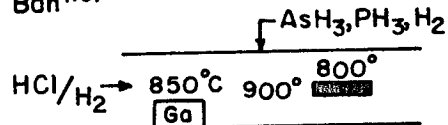
k. Finch and Mehal⁽¹⁶⁾



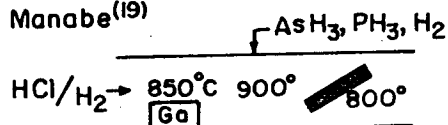
l. Goettler⁽¹⁷⁾



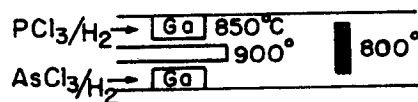
m. Ban⁽¹⁸⁾



n. Manabe⁽¹⁹⁾

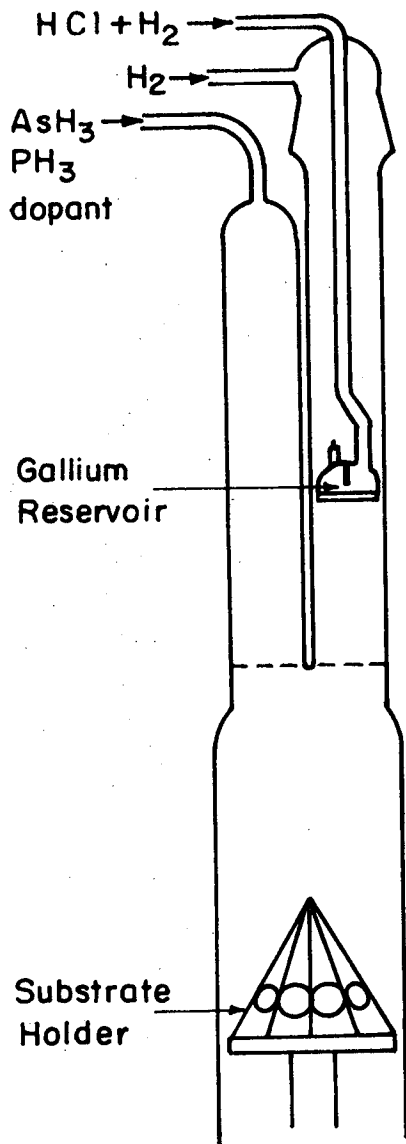


o. Bleicher⁽²⁰⁾

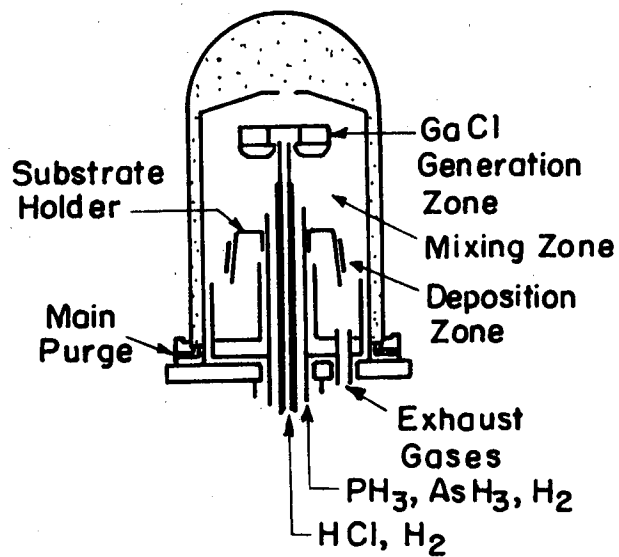


XBL729-6985

Fig. 1



a. Monsanto Reactor



b. AMT Reactor

XBL 729- 7008

Fig. 2

III. THERMODYNAMICS OF PHASE EQUILIBRIA FOR
CHEMICAL VAPOR DEPOSITION OF $\text{GaAs}_{1-x}\text{P}_x$

A. Introduction

Thermodynamic conditions of phase equilibria play an important role in the chemical vapor deposition process setting limits on phase stability, and the direction of chemical reactions. Multiphase equilibria constrain the reaction processes in the gallium saturator and deposition zone of the $\text{GaAs}_{1-x}\text{P}_x$ reactor, while a gas phase equilibrium is established in the gas phase reaction zone of the reactor. The overall feasibility and ultimate efficiency of the chemical vapor deposition process depend on the correctness and availability of thermochemical data for chemical species known to participate in the reactions.

The principles of analysis of multicomponent multiphase equilibria were established early in the development of chemical thermodynamics. J. Willard Gibbs developed a fundamental differential form of the combined first and second laws, known as "Gibbs equation 97,"¹ and also, the celebrated Gibbs phase rule. Equilibria in high temperature gases over solids or liquids have been studied extensively by process metallurgists who developed techniques to establish limits for processes such as the heat treatment of steel.²

Lever³ applied these techniques to equilibria in the Si-H-Cl system important to semiconductor processing. A general analysis of the Ga-As-H-Cl system important in the growth of GaAs from the gas phase was later outlined by Hurle and Mullin.⁴ This approach was followed by Seki and Araki^{5,6} to calculate equilibrium properties of the Ga-P-H-Cl system. Goettler⁷ has also calculated the equilibrium properties of the G-As-H-Cl

system, but calculated diffusion limited growth rates as well. More recently Manabe et al.⁸ and Bleicher⁹ have followed this basic method of analysis to compute equilibria in the Ga-As-P-H-Cl system, important for the growth of $\text{GaAs}_{1-x}\text{P}_x$ alloys by chemical vapor deposition.

In this section the conditions of gas-liquid, gas phase and gas-solid equilibria occurring in the deposition of $\text{GaAs}_{1-x}\text{P}_x$ from $\text{Ga}(\ell)$, $\text{PH}_3(\text{g})$ and $\text{AsH}_3(\text{g})$ precursors will be analyzed using a simplified approach and without losing accuracy to establish criteria of efficiency and feasibility of deposition.

B. Reaction Equilibria in the Ga-As-P-H-Cl System

Chemical reactions equilibria in the Ga-As-P-H-Cl system known to take place in the gas phase and with $\text{Ga}(\ell)$ and $\text{GaAs}_{1-x}\text{P}_x(\text{s})$ alloys are summarized in Table I along with equilibrium constants, K_i and the reactor zone where the equilibrium is expected to apply. The magnitude of $\log K_i$ for these reactions is shown in Fig. 1 over the temperature range expected in the reactor for each of the three reactor zones.

A schematic of the $\text{GaAs}_{1-x}\text{P}_x$ reactor using AsH_3 , PH_3 and $\text{Ga}(\ell)/\text{HCl}$ as reactants in a H_2 carrier gas is shown in Fig. 2. When HCl in H_2 is introduced into a liquid gallium saturator, and the products mixed with AsH_3 and PH_3 , the gas phase species appearing as a result of chemical reaction are shown in Fig. 2 for each of the reactor zones.

By a comparison of the relative magnitudes of the equilibrium constants, the following species can be eliminated at the temperature of interest:

- a. Cl , Cl_2 in the gallium saturator zone
- b. Cl , Cl_2 , AsCl_3 , PCl_3 , in the reaction zone
- c. Cl , Cl_2 , AsCl_3 , PCl_3 , AsH_3 , PH_3 in the deposition zone.

Table I. Reaction equilibria in the Ga-As-P-H-Cl system

Reaction number	Reaction	$\log_{10} K_i$ (atm units)	Zone	Reference
1	$\text{Ga}(\ell) + \frac{1}{2} \text{Cl}_2 \rightarrow \text{GaCl}(\text{g})$	$6.46 + 3.69 \times 10^{-3} / T - 0.47 \ln T$	Saturation	12, 13, 14, 15 (calculated)
2	$\text{Ga}(\ell) + \frac{3}{2} \text{Cl}_2 \rightarrow \text{GaCl}_3(\text{g})$	$-1.96 + 2.25 \times 10^4 / T - 0.17 \ln T$	Saturation	11 (calculated)
3	$\text{GaCl} + \text{Cl}_2 \rightarrow \text{GaCl}_3(\text{g})$	$-8.37 + 1.87 \times 10^4 / T + 0.30 \ln T$	Saturation	11 (calculated)
4	$\text{GaCl}_3 + 2\text{Ga} \rightarrow 3\text{GaCl}(\text{g})$	$4.87 - 4.66 \times 10^3 / T$	Saturation	13 (experimental)
5	$\frac{1}{2} \text{H}_2 + \frac{1}{2} \text{Cl}_2 \rightarrow \text{HCl}(\text{g})$	$2.79 + 4.56 \times 10^3 / T - 0.31 \ln T$	Saturation	12 (calculated)
6	$\text{GaCl}_3 + \text{H}_2 \rightarrow \text{GaCl} + 2\text{HCl}$	$13.95 - 9.58 \times 10^3 / T - 0.92 \ln T$	Saturation	calc. from reactions 3&5
7	$\text{As}_4(\text{g}) \rightarrow 2\text{As}_2(\text{g})$	$11.6 - 1.36 \times 10^4 / T - 0.43 \ln T$	Reaction	13, 15 (calculated)
8	$\frac{1}{4} \text{As}_4 + \frac{3}{2} \text{H}_2 \rightarrow \text{AsH}_3(\text{g})$	$3.65 - 7.52 \times 10^3 / T - 1.0 \ln T + 0.6 \times 10^{-3} T$	Reaction	12, 13, 15 (calculated)
9	$\frac{1}{4} \text{As}_4 + \frac{3}{3} \text{Cl}_2 \rightarrow \text{AsCl}_3$	$-6.18 + 1.76 \times 10^4 / T + 0.37 \ln T$	Reaction	12, 13, 15 (calculated)
10	$\text{Ga}(\ell) + \frac{1}{4} \text{As}_4 \rightarrow \text{GaAs}(\text{s})$	$-4.62 + 6.15 \times 10^3 / T + 0.35 \times 10^{-3} T$	Deposition	12, 13, 16 (calculated)
11	$2\text{GaCl} + \frac{1}{2} \text{As}_4 \rightarrow 2\text{GaAs}(\text{s}) + \text{Cl}_2$	$-21.64 + 4.86 \times 10^3 / T + 1.1 \ln T$	Deposition	12 (calculated)

Table I. (continued)

Reaction number	Reaction	$\log_{10} K_1$ (atm units)	Zone	Reference
12	$3\text{GaCl} + \frac{1}{2}\text{As}_4 \rightarrow 2\text{GaAs} + \text{GaCl}_3$	$-30.1 + 2.36 \times 10^4 / T + 1.4 \ln T + 0.7 \times 10^{-3} T$	Deposition	17 (experimental)
13	$\text{GaCl} + \frac{1}{4}\text{As}_4 + \frac{1}{2}\text{H}_2 \rightarrow \text{GaAs} + \text{HCl}$	$-8.04 + 6.99 \times 10^3 / T + 0.22 \ln T + 0.35 \times 10^{-3} T$	Deposition	18 (experimental)
14	$\text{P}_4 \rightarrow 2\text{P}_2$	$11.5 - 1.21 \times 10^4 / T - 0.5 \ln T$	Reaction	13, 19 (calculated)
15	$\frac{1}{4}\text{P}_4 + \frac{3}{2}\text{H}_2 \rightarrow \text{PH}_3$	$4.88 + 1.47 \times 10^3 / T - 1.2 \ln T$	Reaction	13, 19 (calculated)
16	$\frac{1}{4}\text{P}_4 + \frac{3}{2}\text{Cl}_2 \rightarrow \text{PCl}_3$	$-6.21 + 1.79 \times 10^4 / T + 0.25 \ln T$	Reaction	13, 16, 19 (calculated)
17	$\text{Ga} + \frac{1}{2}\text{P}_2 \rightarrow \text{GaP}$	$-5.36 + 9.41 \times 10^3 / T$	Deposition	20 (experimental)
18	$\text{Ga} + \frac{1}{4}\text{P}_4 \rightarrow \text{GaP}$	$-2.46 + 6.38 \times 10^3 / T - 0.13 \ln T$	Deposition	Calculated from reactions 14 & 17
19	$2\text{GaCl} + \frac{1}{2}\text{P}_4 \rightarrow 2\text{GaP} + \text{Cl}_2$	$-18.00 + 5.39 \times 10^3 / T + 0.68 \ln T$	Deposition	Calculated from reactions 18 & 12
20	$3\text{GaCl} + \frac{1}{2}\text{P}_4 \rightarrow 2\text{GaP} + \text{GaCl}_3$	$-26.46 + 2.41 \times 10^4 / T + 0.98 \ln T$	Deposition	Calculated from reactions 19 & 16
21	$\text{GaCl} + \frac{1}{4}\text{P}_4 + \frac{1}{2}\text{H}_2 \rightarrow \text{GaP} + \text{HCl}$	$-6.08 + 7.255 \times 10^3 / T + 0.03 \ln T$	Deposition	Calculated from reactions 18, 14

Table I. (continued)

Reaction number	Reaction	$\log_{10} K_i$ (atm units)	Zone	Reference
22	$\text{As}_2 + \text{P}_2 \rightarrow \text{As}_2\text{P}_2$	not determined	Reaction	----
23	$\text{As}_2\text{P}_2 \rightarrow 2\text{AsP}$	not determined	Reaction	----
24	$2\text{As}_2\text{P}_2 \rightarrow \text{As}_3\text{P} + \text{AsP}_3$	not determined	Reaction	----
25	$\text{Ga}(\ell) + \text{HCl} \rightarrow \text{GaCl} + \frac{1}{2}\text{H}_2$	$K_{25} = K_1/K_5$	Saturation	Calculated from reactions 1&5
26	$\text{GaCl} + 2\text{HCl} \rightarrow \text{GaCl}_3 + \text{H}_2$	$K_{26} = K_3/K_5^2$	Saturation	Calculated from reactions 3&5

There is currently insufficient data to determine the equilibria with polymers of arsenic and phosphorous. However Ban's study¹⁰ showed that the polymers AsP , As_2P_2 , As_3P , AsP_3 are present. The total concentration of these polymers is about 10-20% of the total of arsenic and phosphorous combined, and should become significant at high temperatures. These polymers are excluded in the present analysis, since in the deposition zone the total component partial pressures of arsenic and phosphorous present do not change significantly during the deposition process.

The calculation of phase equilibria required in the Ga-As-P-H-Cl system requires knowledge of important reacting species, appropriate reaction constants, and conditions for conservation of mass. A measure of the number of system constraints required for equilibrium is the Gibbs phase rule which relates the number of degrees of freedom of a multicomponent, multiphase equilibrium, v , to the number of restrictions r , and the variance n

$$v = n + 2 - r \quad (1)$$

The variance is the number of variables whose values must be assigned in order to specify completely the state of the system. Thus, for the five components Ga, As, P, H and Cl, and two phases (gallium liquid and vapor, or $GaAs_{1-x}P_x$ solid and vapor), $v = 5$. If temperature and pressure are two of the variables held constant, then three additional variables must be constant for equilibrium. If equilibrium in the gas phase alone is considered, $v = 6$, and four constraints are needed in addition to T and P. System properties can then be defined as a function of T, P and the constraints, q_i . Then for any system property we have,

$$\text{system property} = f(P, T, q_1, \dots, q_{v-2}). \quad (2)$$

The constraints can be deduced by requiring conservation of mass for each of the component elements. If m_i denotes the moles of component i while n_j denotes the moles of species j , then for I components and J species the conservation conditions are

$$m_i = \sum_{j=1}^J \alpha_{ij} n_j, \quad i = 1, 2, \dots, I \quad (3)$$

where α_{ij} is the stoichiometric number of components i in species j . Additional constraints are supplied by the reaction equilibria. These are expressed in terms of partial pressures of species i , P_i , or in terms of numbers of moles, by

$$P_j = n_j P \left(\sum_{j=1}^J n_j \right)^{-1} \quad (4)$$

and, therefore,

$$K = f(P_j) \text{ or } K = f(n_j) \quad (5)$$

Finally, the system constraints can be defined on the basis of a fixed total moles by the ratios,

$$q_i = m_i \left(\sum_{i=1}^J m_i \right)^{-1} \quad i = 1, 2, \dots, v-2 \quad (6)$$

In systems where one component, n_I , is in excess, an alternate definition can be made

$$q_i = \frac{n_i}{n_I} \quad (7)$$

The definition of q_i in terms of a species molar ratio has been used in equilibria involving III-V compounds where H_2 is in excess.

To convert to a partial pressure basis, Eqs. (3) and (4) can be combined to give

$$m_i P \left(\sum_{j=1}^J n_j \right)^{-1} = \sum_{j=1}^J \alpha_{ij} P_j \quad (3')$$

The total system moles, $\sum_{j=1}^J n_j$, can be specified by fixing the total system volume V , or alternately for an open system, the total volumetric flow rate, and assuming the ideal gas law as the equation of state for the gas phase. Therefore

$$\sum_{j=1}^J n_j = \frac{PV}{RT} \quad (8)$$

The following composition parameters can then be introduced:

$$q_{Cl} = \frac{P_{HCl} + P_{GaCl} + 3P_{GaCl_3}}{P} = \frac{P^{\circ}_{HCl}}{P} \quad (9)$$

$$q_{As} = \frac{4P_{As_4} + P_{As_2} + \dots}{P} = \frac{P^{\circ}_{AsH_3}}{P} \quad (10)$$

$$q_P = \frac{4P_{P_4} + 2P_{P_2} + \dots}{P} = \frac{P^{\circ}_{PH_3}}{P} \quad (11)$$

It will be seen later that these quantities are conserved throughout the gallium saturation and reaction zones. However a more useful parameter, which is independent of the deposition reaction can be deduced from the above three expressions

$$q_{\text{GaAsP}} = q_{\text{Ga}}^{-x} q_{\text{As}}^{-1-x} q_{\text{P}} \quad (12)$$

This parameter is very useful in determining the equilibria in the deposition zone as this is satisfied by the material balance of species Ga, As and P in the formation of $\text{GaAs}_{1-x}\text{P}_x$.

A general solution to an equilibrium problem in terms of Eqs. (3), (4), and (5), utilizes the following procedure:

1. After eliminating the species which are not present in any great extent relative to majority species, the system's five degrees of freedom can be completely specified by fixing temperature, pressure and flow rates (composition parameters) of AsH_3 , PH_3 and HCl relative to that of H_2 .
2. The system of equations for the equilibrium can be solved by assuming reactions 1, 5 in the gallium saturator zone, reactions 7, 8, 14, 15 in the reaction zone, reactions 3, 7, 13, 14, 21 in the deposition zone (besides the reactions for combination of GaAs and GaP).

C. Gallium Saturation Equilibria

In the saturation zone $\text{Ga}(\ell)$ reacts with HCl and H_2 gas to form volatile gallium compounds, principally GaCl and GaCl_3 . The species present in this zone are Ga, Cl and H, and for $\text{Ga}(\ell)$ -vapor phase equilibrium the Gibbs phase rule requires three constraints for equilibrium e.g., T, P and q_{Cl} . A typical value for the input q_{Cl} , denoted by q_{Cl}^0 is 0.01 corresponding to an HCl partial pressure in the range of 10^{-2} - 10^{-3} atm in H_2 . The majority species present at equilibrium in this zone are GaCl , GaCl_3 , HCl and H_2 . Therefore, in addition

to q_{Cl} , reactions 1, 2, and 5 in Table I and the total pressure constraint (here $P=1$ atm) are sufficient to specify the equilibrium. The resulting system of equations for equilibrium are then

$$q_{\text{Cl}} = P_{\text{HCl}} + P_{\text{GaCl}} + 3P_{\text{GaCl}_3} = q_{\text{Cl}}^{\circ} = P_{\text{HCl}}^{\circ} \quad (13)$$

$$1 = P_{\text{GaCl}} + P_{\text{GaCl}_3} + P_{\text{HCl}} + P_{\text{H}_2} \quad (14)$$

$$\text{Ga}(\ell) + \text{HCl} = \text{GaCl} + \frac{1}{2} \text{H}_2, \quad \frac{K_1}{K_5} = \frac{P_{\text{GaCl}} P_{\text{H}_2}^{1/2}}{P_{\text{HCl}}} \quad (15)$$

$$\text{Ga}(\ell) + 3\text{HCl} = \text{GaCl}_3 + \frac{3}{2} \text{H}_2, \quad \frac{K_2}{K_5^3} = \frac{P_{\text{GaCl}_3} P_{\text{H}_2}^{3/2}}{P_{\text{HCl}}^3} \quad (16)$$

A very good approximation is to assume that the partial pressure of hydrogen is 1 atm. This is a very sound assumption in the region of interest since $P_{\text{HCl}}^{\circ} \sim 10^{-2} - 10^{-3}$ atm. The simplified expressions for equilibrium become,

$$P_{\text{HCl}} = \frac{K_5}{K_1} P_{\text{GaCl}} \quad (17)$$

$$P_{\text{GaCl}_3} = \frac{K_2}{K_5^3} \cdot P_{\text{HCl}}^3 = \frac{K_2}{K_1^3} P_{\text{GaCl}}^3 \quad (18)$$

and

$$\begin{aligned} q_{\text{Cl}}^{\circ} &= \frac{K_5}{K_1} \cdot P_{\text{GaCl}} + 1 P_{\text{GaCl}} + 3 \frac{K_2}{K_1^3} \cdot P_{\text{GaCl}}^3 \\ &= \left(1 + \frac{K_5}{K_1} \right) \cdot P_{\text{GaCl}} + 3 \frac{K_2}{K_1^3} \cdot P_{\text{GaCl}}^3 \end{aligned} \quad (19)$$

These three equations can be combined to give a single equation in the variable p_{GaCl}

$$p_{\text{GaCl}}^3 + C_1 p_{\text{GaCl}} + C_2 \cdot q_{\text{Cl}}^\circ = 0 \quad (20)$$

On solving this equation by iteration, one finds at 850°C the following magnitudes for p_{GaCl} , p_{GaCl_3} and p_{HCl} in equilibrium for $p_{\text{HCl}}^\circ = 0.01 \text{ atm}$,

$$p_{\text{GaCl}} = 0.995 p_{\text{HCl}}^\circ \cong 10^{-2} \text{ atm}$$

$$p_{\text{HCl}} = 0.005 p_{\text{HCl}}^\circ = 5 \times 10^{-5} \text{ atm} \quad (21)$$

$$p_{\text{GaCl}_3} = 10^{-6} \times p_{\text{HCl}}^\circ = 10^{-8} \text{ atm}$$

and therefore

$$p_{\text{H}_2} = 0.99 \text{ atm.}$$

These sample calculations show that virtually all of the HCl fed into this zone is converted to GaCl and that GaCl₃ is only present at many orders of magnitude less than GaCl₁. This is a strong proof that GaCl is the primary gallium compound reacting in the deposition process.

Another conclusion which can be drawn here is that the HCl conversion at equilibrium is essentially 100%; thus, with a properly designed saturator, all the HCl can be utilized for growth in the form of GaCl. Excess HCl can be introduced, however, by designing a saturator with fractional efficiency, or introduced separately beyond the saturator.

Another great advantage of designing the saturator to produce equilibrium is that the conversion of HCl to GaCl is independent of temperature in the range of 750-900°C. Therefore the saturator temperature does not affect the conversion efficiency to any great extent and the temperature of gallium boat need not be regulated to any great precision. This fact is very important for a large gallium saturator since it is difficult to maintain a uniform temperature over a long distance without costly furnace design.

D. Reaction Zone Equilibria

In the reaction zone the output from the saturator is mixed with an input PH_3 , AsH_3 , H_2 mixture, and three events take place:

1. Heating of the arsine-phosphine-hydrogen stream and the gallium saturator output stream to the reaction temperature,
2. decomposition of arsine and phosphine
3. mixing of the decomposition products by turbulent flow through orifices.

The temperature in this zone is higher than that of the saturation zone so that the equilibrium for products of the gallium saturator will change only slightly. Earlier studies¹⁰ have indicated that no reaction takes place between GaCl and arsenic or phosphorous in this region possibly due to the absence of any nucleating surface. Therefore, the only reactions taking place in the reaction zone are reactions 7, 8, 14 and 15 in Table I.

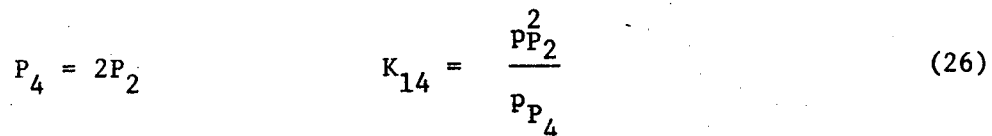
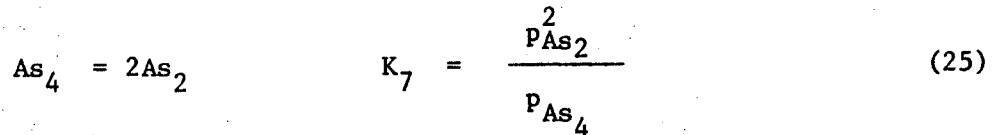
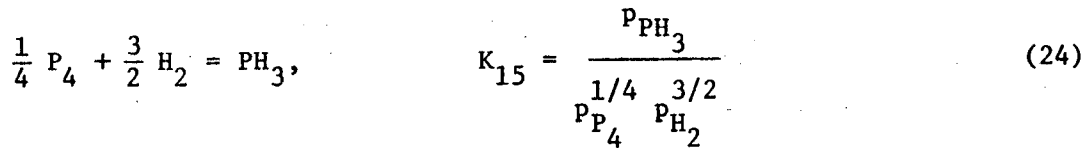
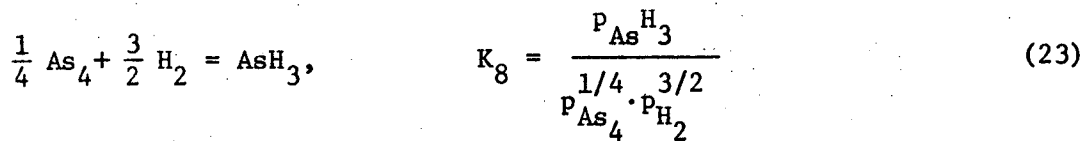
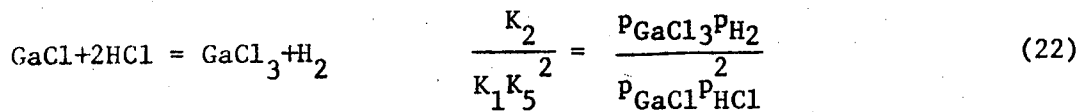
The gaseous species existing in this zone are GaCl, GaCl₃, AsH₃, H₂, HCl, PH₃, P₂, P₄, As₂, As₄ and for gas phase equilibria the Gibbs phase rule

requires that four composition variables, one for each of the gas phase species, be specified in addition to T and P.

The polymer species AsP , As_3P , AsP_3 and As_2P_2 should also be taken into account, but the lack of sufficient thermodynamic data prevents this. However, it can be estimated that the combined entropies of reaction for reactions 22, 23 and 24 in Table I are near zero since the number of bonds broken on one side of each reaction equation equals the number of bonds formed on the other, and since the vibrational and rotational mode energies for the tetramers is only slightly less than that of the dimers. The polymers reaction equilibria should therefore change slowly with temperature in the gas phase. This contention is supported by the similar reactions $2P_2 \rightleftharpoons P_4$ and $2As_2 \rightleftharpoons As_4$ whose reaction constants (K_{14} and K_7 respectively in Table I) change slowly with temperature.

The significant gaseous species, neglecting As-P polymers, are HCl, AsH_3 , PH_3 , P_4 , P_2 , As_4 , As_2 , H_2 , GaCl and $GaCl_3$. For ten unknowns, we require ten equations. These are obtained from reactions 7, 8, 14, 15 in Table I, from the composition constraints, q_{As} , q_P , q_{Ga} , and q_{Cl} , and the total pressure constraints. The solving equations are then,

-35-



$$q_{\text{As}} = P_{\text{AsH}_3}^\circ = P_{\text{AsH}_3} + 4p_{\text{As}_4} + 2p_{\text{As}_2} \quad (27)$$

$$q_{\text{P}} = P_{\text{PH}_3}^\circ = P_{\text{PH}_3} + 4p_{\text{P}_4} + 2p_{\text{P}_2} \quad (28)$$

$$q_{\text{Ga}} = 0.995 P_{\text{HCl}}^\circ = P_{\text{GaCl}} + P_{\text{GaCl}_3} \quad (29)$$

$$q_{\text{Cl}} = P_{\text{HCl}}^\circ = P_{\text{HCl}} + P_{\text{GaCl}} + 2p_{\text{GaCl}_3} \quad (30)$$

and

$$1 = P_{\text{AsH}_3} + p_{\text{PH}_3} + p_{\text{P}_4} + p_{\text{P}_2} + p_{\text{As}_4} + p_{\text{As}_2} + p_{\text{GaCl}} + p_{\text{GaCl}_3} + p_{\text{HCl}} + p_{\text{H}_2}. \quad (31)$$

It can be shown from these equations that arsenic and phosphorous equilibria are totally independent of each other and hence separately solvable.

Arsenic equilibria, can be calculated from Eqs. 23, 25 and 27. Upon combining these equations, and simplifying, we obtain

$$P_{As_4} + \frac{K_7^{1/2}}{2} P_{As_4}^{1/2} + \frac{K_8}{4} P_{As_4}^{1/4} - \frac{1}{4} q_{As} = 0 \quad (32)$$

from which it follows that, at 900°C,

$$\begin{aligned} P_{As_4} &\cong \frac{1}{4} q_{As} \\ P_{As_2} &\cong \frac{1}{2} q_{As} \times 10^{-3} \\ P_{AsH_3} &\cong q_{As} \times 10^{-7}. \end{aligned} \quad (33)$$

From this calculation, it is apparent that most of the arsine is converted to As_4 , the tetramer rather than the dimer.

Phosphorous equilibria is calculable from Eqs. 29, 26, 28. The equations are combined in a similar manner to that for arsenic to solve for a single partial pressure unknown. At 900°C, the partial pressures of phosphorous polymers are,

$$P_{P_4} = \frac{1}{4} q_p \times 0.99$$

$$P_{P_2} = \frac{1}{2} q_p \times 10^{-2}$$

$$P_{PH_3} = q_p \times 10^{-4}$$

Again the tetramer is the majority phosphorous component. Although the magnitude of P_2 and PH_3 are higher than those of As_2 and AsH_3 they are safely negligible at this temperature.

In conclusion, virtually all of arsine is converted to As_4 in the reaction zone and all phosphine converted to P_4 . The unassessed partial pressure of As_2P_2 should be similar, be large compared to that of AsP . Therefore, in spite of the large number of group V polymers, only the tetramers enter the deposition zone making the solution of gas phase equilibria in that zone easier. These majority gas species leaving the reaction zone are then H_2 , $GaCl$, As_4 , P_4 , and probably As_2P_2 .

E. Deposition Zone Equilibria

This is by far the most important phase equilibrium in the reactor, and also the most difficult to calculate. The analysis of equilibria in the gallium saturation zone and the reactor zone show that only certain gaseous species enter this zone. Once in contact with solid $\text{GaAs}_{1-x}\text{P}_x$, however, other species can appear in quantities which can affect the rate of deposition of solid, as will be shown in Chapter IV. The analysis of equilibria at the solid-gas interface will enable us to predict the driving forces for deposition, the composition of the alloy solid and the effects of various parameters on the growth rates, e.g. temperature and flow rates of input gases.

As shown earlier, the gases entering this zone are principally H_2 , GaCl , As_4 , P_4 and traces of other species. But once the gases come into contact with the solid substrate, the gas phase composition changes by selective evaporation of the solid, or condensation. It will be shown that the possible gaseous species which exist in this region are H_2 , HCl , GaCl , GaCl_3 , As_4 , As_2 , P_4 , P_2 , besides the polymers of arsenic and phosphorous, neglected here.

The Gibbs phase rule for species Ga, As, P, Cl and H, and for vapor and solid phases gives a variance of five, requiring that T, P, and three composition functions be held constant for equilibrium. The eight unknowns, however, require eight equations to solve the equilibrium problem. An additional unknown is x in the compound $\text{GaAs}_{1-x}\text{P}_x$, requiring a ninth equation. The required equations are given by reactions 7, 14, 13, 21, 3 in Table I, the composition parameters q_{Cl} and q_{GaAsP} , the

ratio of phosphorus to arsenic in the gas phase, q_{P+As} and an independent expression for x deduced from the activities of the group V elements in the solid, a_{GaAs} and a_{GaP} . The required set of equations are then,

$$P_4 = 2P_2, \quad K_{14} = p_P^2 \cdot p_{P_4}^{-1} \quad (35)$$

$$As_4 = 2As_2, \quad K_7 = p_{As_2}^2 \cdot p_{As_4}^{-1} \quad (36)$$

$$GaCl + 2HCl = GaCl_3 + H_2, \quad K_3/K_5^2 = p_{GaCl_3} p_{H_2}^{-1} p_{GaCl}^{-2} p_{HCl}^{-2} \quad (37)$$

$$GaCl + \frac{1}{4}As_4 + \frac{1}{2}H_2 = GaAs(s) + HCl, \quad K_{13} = p_{HCl}^{-1} p_{GaCl}^{-1/4} p_{As_4}^{-1/4} p_{H_2}^{-1/2} \quad (38)$$

$$GaCl + \frac{1}{4}P_4 + \frac{1}{2}H_2 = GaP(s) + HCl, \quad K_{21} = p_{HCl}^{-1} p_{GaCl}^{-1/4} p_{P_4}^{-1/4} p_{H_2}^{-1/2} \quad (39)$$

$$q_{Cl} = p_{HCl}^{\circ} = p_{GaCl} + 3p_{GaCl_3} + p_{HCl} \quad (40)$$

$$q_{GaAsP} = 0.995 p_{HCl}^{\circ} - p_{AsH_3}^{\circ} - p_{PH_3}^{\circ} \quad (41)$$

$$= p_{GaCl} + p_{GaCl_3} - 4p_{P_4} - 4p_{As_4} - 2p_{P_2} - 2p_{As_2}$$

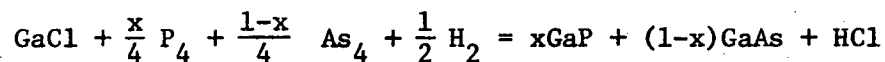
$$q_{AsP} = \frac{p_{PH_3}^{\circ}}{p_{PH_3}^{\circ} + p_{AsH_3}^{\circ}} = \frac{4p_{P_4} + 2p_{P_2} + p_P^s}{4(p_{P_4} + p_{As_4}) + 2(p_{P_2} + p_{As_2}) + p_P^s + p_{As}^s} \quad (42)$$

where p_P^s and p_{As}^s are defined as the partial pressures of phosphorous and arsenic equivalent to the amount of these components in the solid

$GaAs_{1-x}P_x$. The expression for x can be deduced from reactions

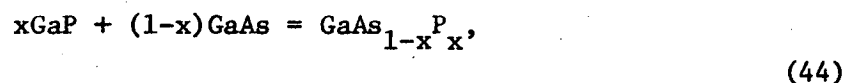
13 and 21 in Table I, and the activities a_{GaAs} and a_{GaP} . If the fraction

x of reaction 21 is added to the fraction (1-x) of reaction 13, the following reaction equation results:



$$\Delta F = x\Delta F_{21} + (1-x)\Delta F_{13}, \quad (43)$$

where $\Delta F_i = -RT \ln K_i$ the free energy change for the reaction. To this equation must be added the free energy of mixing of the alloy



$$\Delta F = RT[x \ln a_{\text{GaP}} + (1-x) \ln a_{\text{GaAs}}]$$

Since the alloys of III-V compounds are known to be regular, the activities can be expressed in terms of x by a regular solution model:

$$a_{\text{GaP}} = x \exp[\alpha(1-x)^2/RT] \quad (45)$$

$$a_{\text{GaAs}} = (1-x) \exp[\alpha x^2/RT].$$

The heat of mixing coefficient α has been calculated by Huber¹¹ (Bleicher, Ref. #15) to be 1 kcal/mole, and consequently the ratio $\alpha/RT \ll 1$, for temperatures near 100°C. The equilibrium constant for the sum of reactions given in Eqs. 43 and 44 is

$$K_{21}^x K_{13}^{(1-x)} = \frac{a_{\text{GaP}}^x a_{\text{GaAs}}^{1-x} P_{\text{HCl}}}{P_{\text{GaCl}} P_{\text{P}_4}^{x/4} P_{\text{As}_4}^{(1-x)/4} P_{\text{H}_2}^{1/2}} \quad (46)$$

And finally, the implicit expression for x is

$$x = \frac{\ln \left[K_{13}^{-1} a_{\text{GaAs}} P_{\text{HCl}} P_{\text{GaCl}}^{-1/4} P_{\text{As}_2}^{-1/2} P_{\text{H}_2}^{-1/2} \right]}{\ln \left[\left(\frac{K_{12}}{K_{13}} \right) \left(\frac{a_{\text{GaAs}}}{a_{\text{GaP}}} \right) \left(\frac{P_{\text{P}_4}}{P_{\text{As}_4}} \right)^{1/4} \right]} \quad (47)$$

A very good assumption for initial estimates is to neglect the gaseous species GaCl_3 altogether and set $P_{\text{GaCl}_3} = 0$. The pressure of GaCl_3 does not exceed 10^{-6} atm at typical conditions whereas the pressures of GaCl and arsenic, etc. are on the order of 10^{-2} atm. By substituting $P_{\text{GaCl}_3} = 0$ and eliminating p_{As_2} , p_{P_4} , p_{P_2} from Eqs. in Eq. 41, the following equation is obtained:

$$q_{\text{GaAsP}} = P_{\text{GaCl}}^{-4} \left[1 + \left(\frac{K_{13}}{K_{21}} \right)^4 \right] p_{\text{As}_4}^{-2} \left[K_7^{1/2} + K_{14}^{1/2} \left(\frac{K_{13}}{K_{21}} \right)^2 \right] p_{\text{As}_4}^{1/2} \quad (48)$$

Alternately this equation can be written as

$$q_{\text{GaAsP}} = P_{\text{GaCl}}^{-4} - A p_{\text{As}_4} - B p_{\text{As}_4}^{1/2} \quad (49)$$

where

$$A = 4 \left[1 + \left(\frac{K_{13}}{K_{21}} \right)^4 \right]$$

$$B = 2 \left[K_7^{1/2} + K_{14}^{1/2} \left(\frac{K_{13}}{K_{21}} \right)^2 \right]$$

Then solving Eq. 49 for $p_{\text{As}_4}^{1/2}$, we obtain

$$p_{\text{As}_4}^{1/2} = \frac{1}{2A} \left\{ \sqrt{B^2 - 4 A q_{\text{GaAsP}} + 4 A p_{\text{GaCl}}^{-4}} - B \right\} \quad (50)$$

A simple equation in P_{GaCl} is finally obtained by substituting Eq. 50 in Eq. 38 and simplifying with the help of Eq. 40 :

$$f = P_{\text{GaCl}} \left[\pm \sqrt{B^2 - 4A q_{\text{GaAsP}} + 4A P_{\text{GaCl}} - B} \right]^{1/2} + \frac{\sqrt{2A}}{K_{13}} \left(P_{\text{GaCl}}^{-q_{\text{Cl}}} \right) \quad (51)$$

Equation 51 can now be solved iteratively for p_{GaCl} .

A and D are functions of temperature which is held constant, as are only q_{Cl} and q_{GaAsP} , which are determined by the initial conditions of gas flow to the reactor.

The equilibria of gases as well as value of x can now be determined from p_{GaCl} by substitution. This approach allows a direct solution which is easier to calculate than a simultaneous set of non-linear equations, yet the accuracy of the calculation is maintained. One parameter can be varied at a time with the others kept constant to examine its effects on the equilibrium.

A set of sample calculations is given in the Appendix 1. Once the values of major species concentrations are known, those of minor species are calculated easily to provide a basis for iterative calculation of the major species. However only one iteration is necessary as the effect of minor components is not greater than 1 percent on major species.

F. Results and Discussion

The conditions for phase equilibria and methods of calculation outlined above permit an assessment of equilibrium partial pressures of the gas phase species throughout the $\text{GaAs}_{1-x}\text{P}_x$ reactor utilizing arsine, phosphine and liquid gallium as source chemicals. When H_2 carrier gas is the majority species, the halide reactant HCl is almost completely converted to GaCl in the gallium saturator. Therefore, unless additional HCl gas is added after the saturator, the reaction zone will contain principally H_2 , GaCl and the arsine and phosphine decomposition products As_4 and P_4 , and in addition the minor species HCl , P_2 , As_2 , GaCl_3 and other group V compounds. By far, the most complex equilibrium is the gas-solid equilibrium in the deposition zone, and the deposition rate and efficiency will depend strongly on this equilibrium in relation to the simpler reaction zone equilibrium. Consequently it is important to examine the gas-solid equilibrium in detail.

Figures 3 to 7 summarize the results of the computational method outlined in section E above for the gas solid equilibrium with $\text{GaAs}_{1-x}\text{P}_x$. In Figs. 3a,b,c the partial pressures of gas phase species in equilibrium with the solid are plotted versus temperature for a fixed value of q_{Cl} corresponding to the conditions q_{GaAsP} , less than, equal to and greater than zero. These figures show the following:

1. p_{P_4} is always less than p_{P_2} at these conditions whereas in the reaction zone gases P_4 is by far the majority species.
2. The initial partial pressure $p_{\text{As}_4}^\circ$ required to maintain $p_{\text{As}_4}^{\text{eq}}$ becomes larger than 0.01 at temperatures above 850°C .

3. When $p_{\text{HCl}}^{\circ} > (p_{\text{AsH}_3}^{\circ} + p_{\text{PH}_3}^{\circ})$, $p_{\text{As}_4}^{\text{eq}}$ is less than $p_{\text{As}_4}^{\circ}$ for a larger range of temperature than when $p_{\text{HCl}}^{\circ} = p_{\text{PH}_3}^{\circ} + p_{\text{AsH}_3}^{\circ}$ and this allowed temperature range is still larger than for the case when

$$p_{\text{HCl}}^{\circ} < p_{\text{PH}_3}^{\circ} + p_{\text{AsH}_3}^{\circ}$$

From this information, we conclude that it is better to operate in the range where $p_{\text{HCl}}^{\circ} > p_{\text{PH}_3}^{\circ} + p_{\text{AsH}_3}^{\circ}$ for a greater control of alloy composition; otherwise the alloy is simply GaP since no deposition of arsenic can occur. This conclusion is also reached by the fact that the $p_{\text{P}_4}^{\text{eq}}$ is very low as compared to $p_{\text{As}_4}^{\text{eq}}$ when $p_{\text{P}_4}^{\circ}$ and $p_{\text{As}_4}^{\circ}$ have the same order of magnitude. The main reason for this behavior is that $K_{13} > K_{21}$ and the ratio to the fourth power is taken in equilibrium calculations. Thus, the difference between arsenic and phosphorous partial pressures can be up to 2-3 orders of magnitude. Since phosphorous tends to react more completely with gallium than arsenic. It is preferable to hold $p_{\text{PH}_3}^{\circ} > p_{\text{AsH}_3}^{\circ}$ e.g., $q_{\text{AsP}} < 0.2$. This conclusion agrees with that reached by Bleicher¹⁰ for $\text{GaAs}_{1-x}\text{P}_x$ deposition from group V chlorides.

Figure 4 shows the effect of temperature on x, where x is the fraction of phosphorous in the alloy $\text{GaAs}_{1-x}\text{P}_x$, through Eq. 47. Curves in the figure correspond to the three cases q_{GaAsP} less than, equal to and greater than zero. Clearly, when q_{GaAsP} is less than zero a slower increase in x is obtained with temperature than with the other two cases. It is also seen that at temperatures below 750°C, there is not much change in x with changing gas phase composition. This is a very important property if the temperatures of operation can be chosen in that range. It will be shown later, however, that for maximizing

growth rates, the temperature must be near 800°C where the change in x with a change in gas composition is much larger.

Another important result obtained from Fig. 4 is that a very precise control over the substrate temperature is required in order to produce deposited layers of uniform composition. This is a very critical problem of current chemical vapor deposition technology.

The requirement of precise temperature control can be circumvented. Consider the dependence of x on the parameter q_{AsP} as shown in Figs. 5a,b,c. These figures further strengthen the conclusion that a very rapid change in the alloy composition takes place with a slight change in temperature or in the ratio of arsine to phosphine. However the change with arsine to phosphine ratio is not large for $x < 0.2$, and particularly for temperatures between 800 and 850°C. This is a very important conclusion as one alloy composition important in device applications is $x = 0.19$. For this particular composition, slight changes in flow rates of incoming gases or temperature of the substrate do not significantly affect the composition of the alloy.

Another point of interest brought out by these figures is that for an alloy composition of $x = 0.2$, $q_{AsP} \cong 0.1$. This again indicates that the arsine flow should always be in excess of the stoichiometric amount for a particular composition of the alloys.

Lastly for q_{GaAsP} increasing from negative to positive values, the composition of the alloy becomes more sensitive to temperature and gas composition dependence of p_{HCl}^0 . Thus, GaCl should always be in excess of the stoichiometric amount required to react with arsenic and phosphorous to form the alloy $GaAs_{1-x}P_x$.

Another interesting aspect of the thermodynamic analysis is the determination of the excess HCl required over the theoretical amount required for equilibrium for fixed T and q_{AsP} . Figures 6a,b,c summarize the results of these calculations and show the effect of q_{Cl} dependence of equilibrium partial pressures of the gas phase on q_{Cl} for fixed values of arsine and phosphine inlet flows at 750, 800, 850°C respectively.

As can be seen from these plots, the equilibrium pressures of arsenic (both tetramer and dimer) and phosphorous (both tetramer of dimer) reach a minimum at a value of q_{Cl} which increases with increasing temperature. This behavior of the equilibrium pressures is significant in affecting the efficiency of the deposition from the gas phase and can be explained through the properties of Eq. (51). The first term in this equation has positive and negative roots. The positive root is required for the solution at lower values of q_{Cl} but as q_{Cl} increases $B^2 = 8Aq_{GaAsP}$ becomes negative and hence the negative root is required in this range. As the transition takes place from one root to the other, the function passes through a minimum. The minimum value of P_i^{eq} at a given temperature for a certain q_{Cl} corresponds to maximum efficiency of deposition for the group V species. This value of q_{Cl} is termed $q_{Cl(max)}$, and shown plotted against temperature of the substrate. (Fig. 7). The figure provides a means for estimating the inlet flow rates of HCl needed to obtain maximum deposition at a certain temperature.

For the particular case plotted, i.e. $p_{AsH_3}^{\circ} = 0.008$ atm and $p_{PH_3}^{\circ} = 0.002$ atm, the $q_{Cl(max)}$ increases greatly between temperatures 750-800°C. It is seen that the excess of HCl required is at least 100% (at 700°C) and increases to about 500% at 850°C. This result is

supported by the fact that experimentalists have emphasized the requirement that HCl be in excess of the stoichiometric amounts in research, as well as commercial reactors.^{10,12}

In summary, the following conclusions can be made for the phase equilibrium properties of the GaAs_{1-x}P_x reactor:

1. Temperature variations of the substrate, and changes in flow rates of the gases will greatly affect the composition of the alloy deposited.
2. The HCl flow to the gallium saturator should be used in excess of the stoichiometric amount required for reacting with arsine and phosphine for efficient utilization of the group V components. The exact excess can be estimated at various temperatures, but varies greatly with the temperature of the substrate.
3. Temperatures above 850°C will result in the growth of GaP for $P_{HCl}^{\circ} > P_{AsH_3}^{\circ} + P_{PH_3}^{\circ}$ due to the high value of $P_{As_4}^{eq}$ above that temperature.
4. Arsine should always be in excess of the arsenide fraction desired in the alloy solid, i.e. for $x = 0.2$ q_{AsP} should be nearly 0.1.
5. The presence of the minority species (i.e., GaCl₃, Cl, Cl₂) do not significantly affect the equilibrium calculations of phase equilibria.

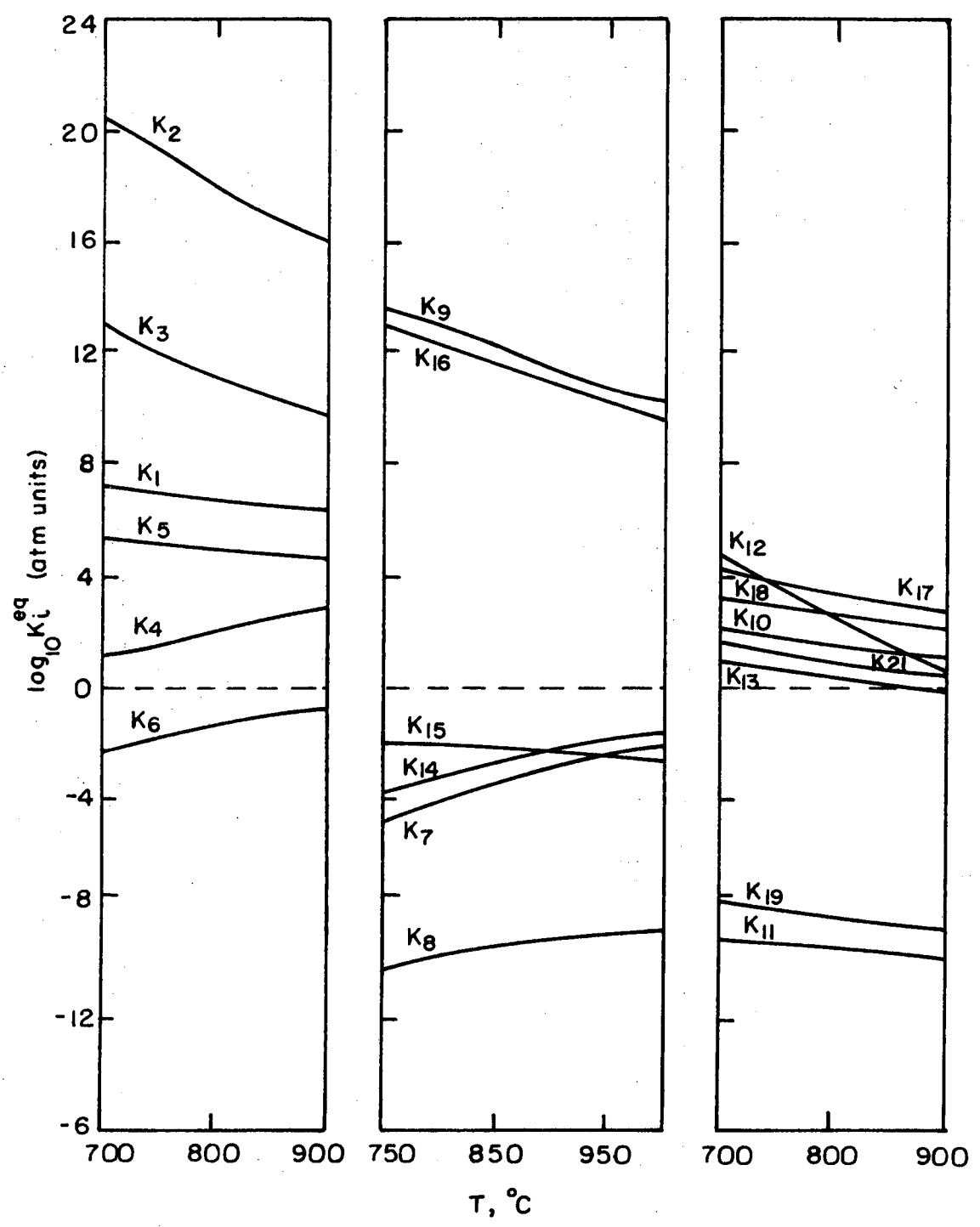
BIBLIOGRAPHY

1. The Collected Works of J. Willard Gibbs, Vol. I. (Longman, Green and Co., Inc., N. Y., 1931).
2. R. W. Garry, Trans. AIME 188, 671 (1950).
3. R. F. Lever, IBM Research and Development 8, 460 (1964).
4. D. T. J. Houle and J. B. Mullin, J. Phys. Chem. Solids, Supplement 1, 241 (1966).
5. H. Seki and H. Avaki, Japan J. Appl. Phys. 6, 1414 (1967).
6. H. Seki, et al., Japan J. Appl. Phys. 7, 1324 (1968).
7. L. A. Goettler, "Diffusion and Surface Kinetics in Epitaxial Vapor of Deposition of GaAs," AIChE 67th National Meeting, February 1970.
8. T. Manabe, "Thermodynamic Analysis of the Ga-As-P-Cl-H System for Vapor Growth of GaAs_{1-x}P_x," Third International Conference on CVD, April 1972, pp. 25-36.
9. M. Bleicher, J. Electrochem. Soc. 111, 585 (1964).
10. V. Ban, J. Electrochem. Soc. 118, 1473 (1971).
11. D. Huber, Ref. 15, Bleicher, J. Electrochem. Soc. 119, 613 (1972).
(Private communication)
12. R. Fargusson and T. Gabor, J. Electrochem. Soc. 111, 585 (1964).
13. "Contribution to the Data on Theoretical Metallurgy," U. S. Dept. of Commerce, Bureau of Mines, Bulletin 584 (1960).
14. L. Quill, Chemistry and Metallurgy of Miscellaneous Materials, (McGraw-Hill Book Co., Inc., New York, 1950).
15. D. R. Stull and G. C. Sinke, Advan. Chem. sec. 18 (1956).
16. Chemical Engineers' Handbook, edited by R. Perry, 4th edition, (McGraw-Hill Book Co., Inc., N. Y. 1963).

17. D. J. Kirwan, J. Electrochem. Soc. 117, 1572 (1970).
18. M. Zengel, J. Electrochem. Soc. 112, 1153 (1965).
19. F. Rossini, "Selected Values of Thermodynamic Properties," National Bureau of Standards, Circ. 500 (1952).

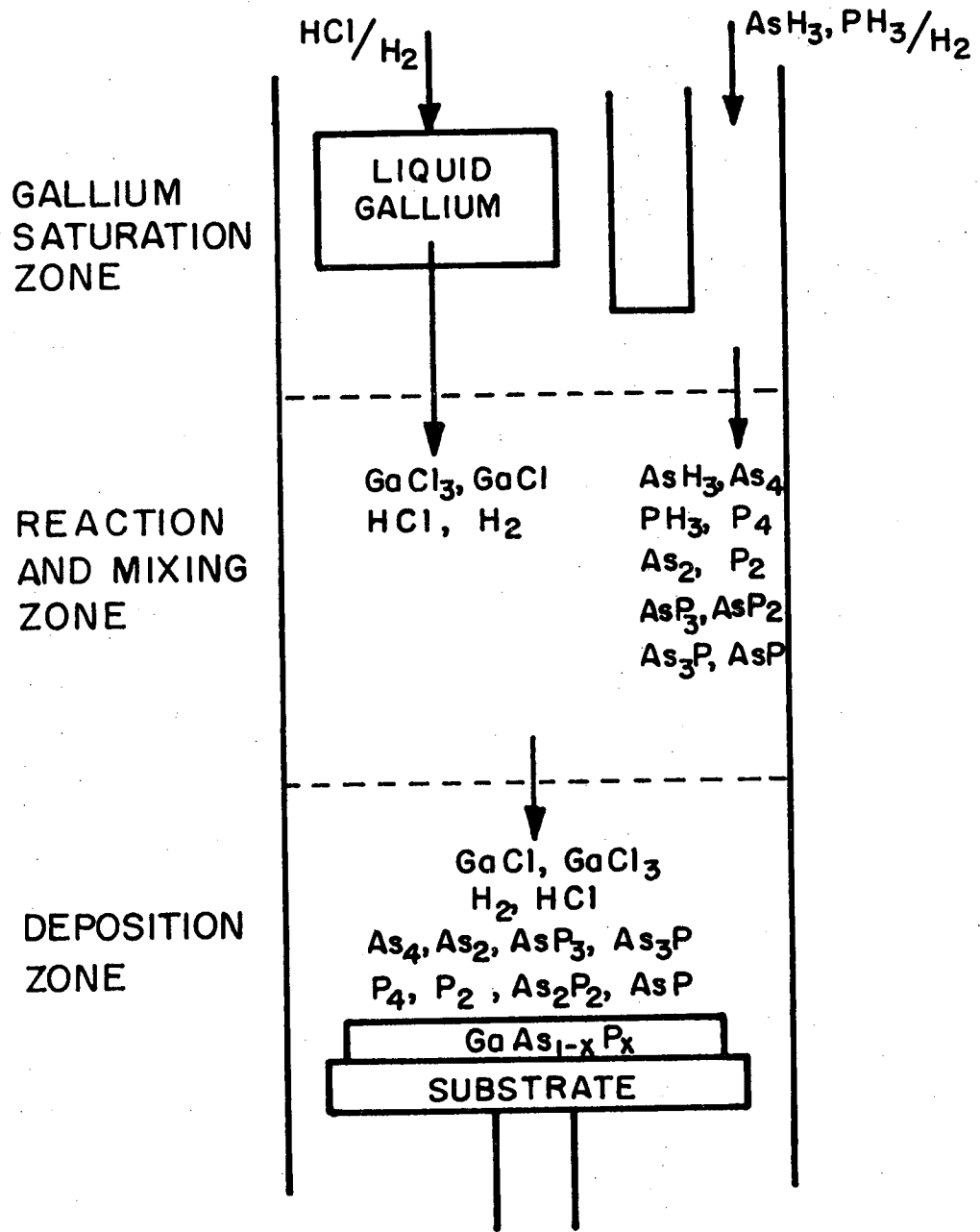
Figure Captions

- Fig. 1. Dependence of reaction equilibrium constants in the Ga-As-P-Cl-H system on temperature.
- Fig. 2. Schematic of the $\text{GaAs}_{1-x}\text{P}_x$ reactor utilizing arsine, phosphine and gallium source chemicals with HCl/H_2 transport. Major gaseous species are shown in each zone.
- Fig. 3. Partial pressures of gaseous species in equilibrium with $\text{GaAs}_{1-x}\text{P}_x$ as a function of temperature.
- a) $q_{\text{Cl}} = 0.01$, $q_{\text{GaAsP}} = 0.002$, $q_p^\circ/\text{P+As} = 0.250$
 - b) $q_{\text{Cl}} = 0.01$, $q_{\text{GaAsP}} = \text{zero}$, $q_p^\circ/\text{P+As} = 0.200$
 - c) $q_{\text{Cl}} = 0.01$, $q_{\text{GaAsP}} = -0.002$, $q_p^\circ/\text{P+As} = 0.167$
- Fig. 4. Dependence of x in $\text{GaAs}_{1-x}\text{P}_x$ on temperature.
- Fig. 5. Dependence of x in $\text{GaAs}_{1-x}\text{P}_x$ on $p_{\text{PH}_3}^\circ/p_{\text{PH}_3}^\circ + p_{\text{AsH}_3}^\circ$, for fixed temperature and
- a) $q_{\text{Cl}} = 0.01$, $q_{\text{GaAsP}} = 0.002$,
 - b) $q_{\text{Cl}} = 0.01$, $q_{\text{GaAsP}} = 0$
 - c) $q_{\text{Cl}} = 0.01$, $q_{\text{GaAsP}} = -0.002$.
- Fig. 6. Partial pressures of gaseous species in equilibrium with $\text{GaAs}_{1-x}\text{P}_x$ as a function of the input HCl partial pressure at $q_p^\circ/\text{P+As} = 0.20$
- a) $T = 750^\circ$
 - b) $T = 800^\circ\text{C}$
 - c) $T = 850^\circ\text{C}$.
- Fig. 7. Dependence of the input partial pressures of HCl corresponding to maximum efficiency of group V elements deposition on temperature.



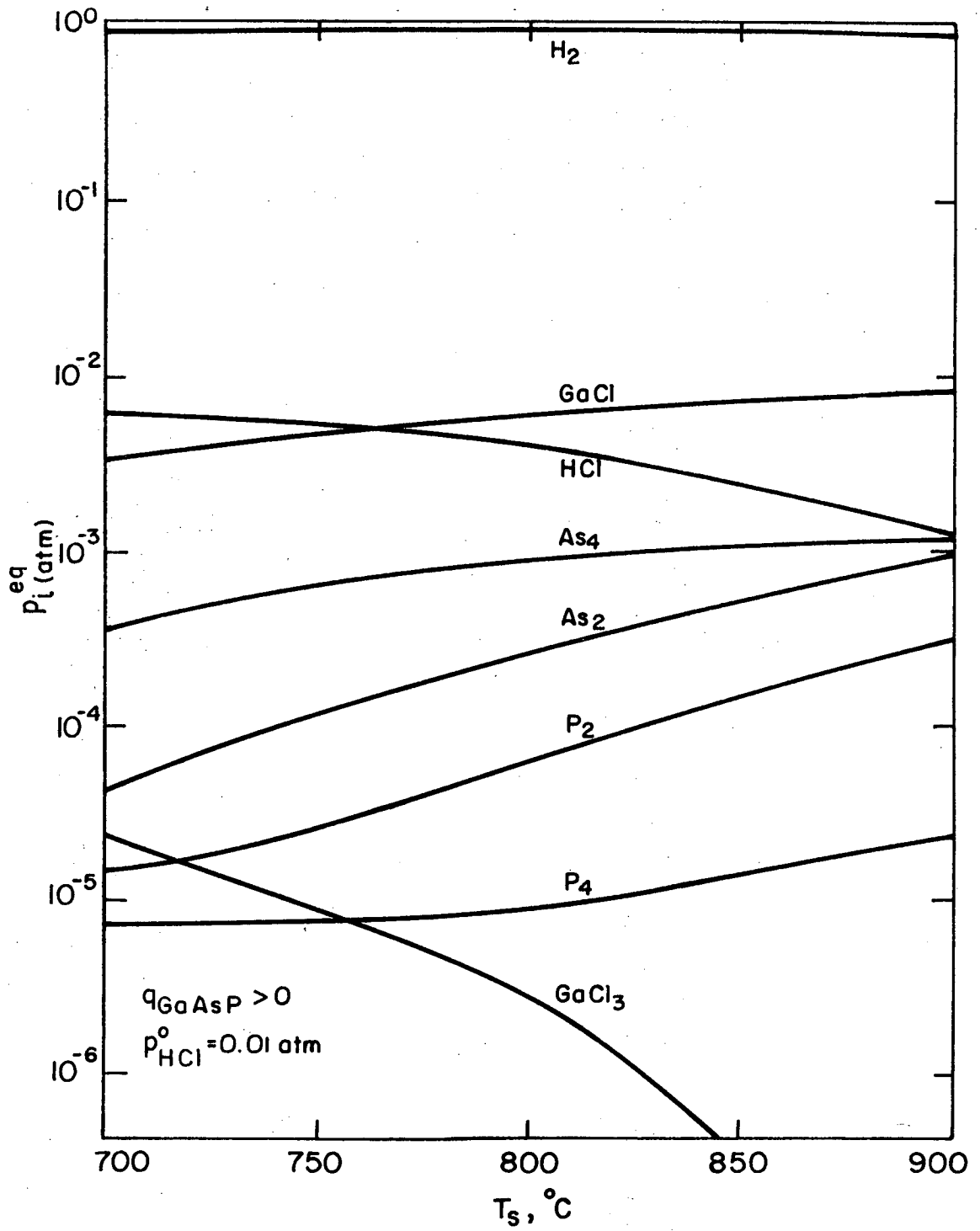
XBL729-7009

Fig. 1



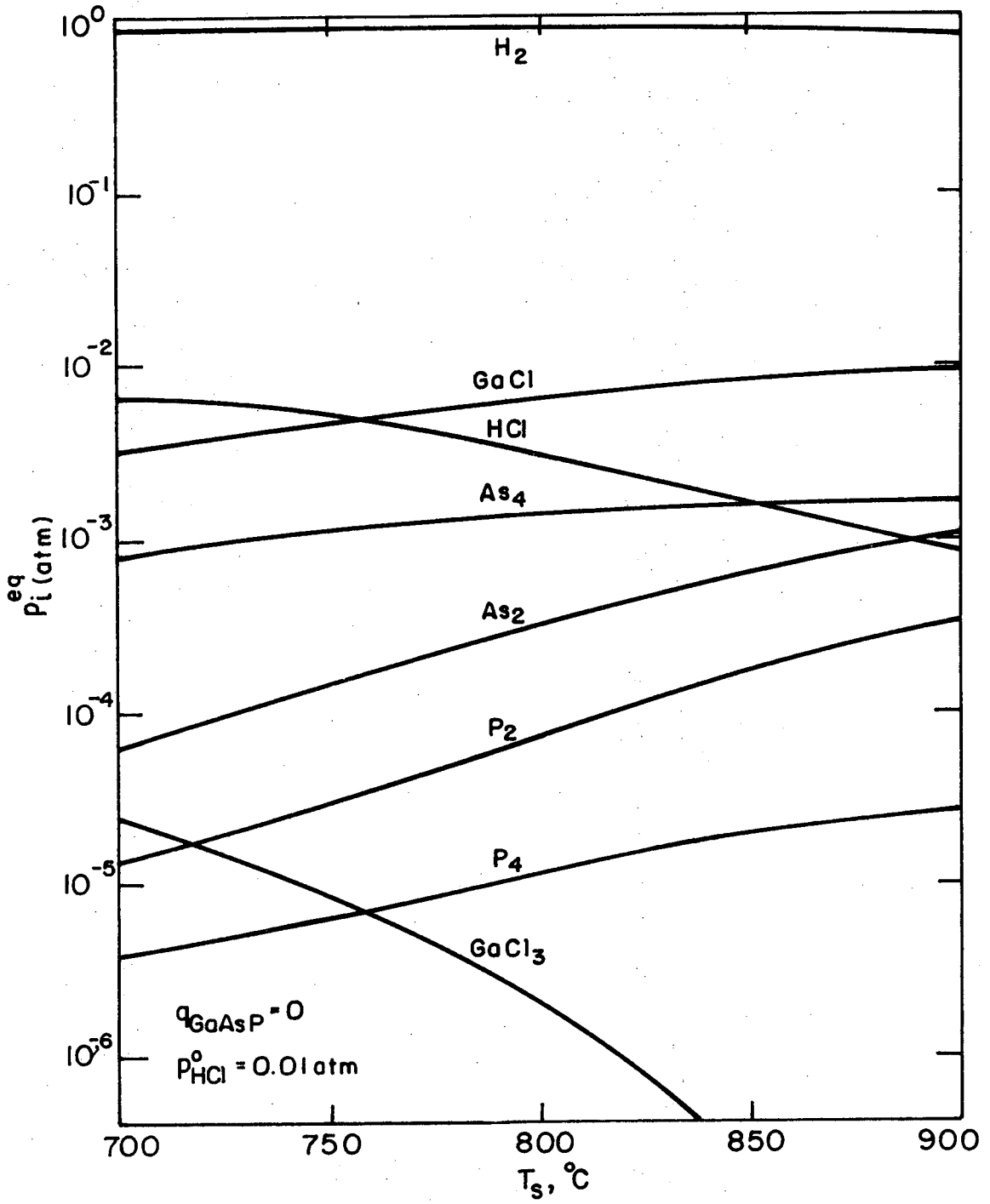
XBL729-6986

Fig. 2



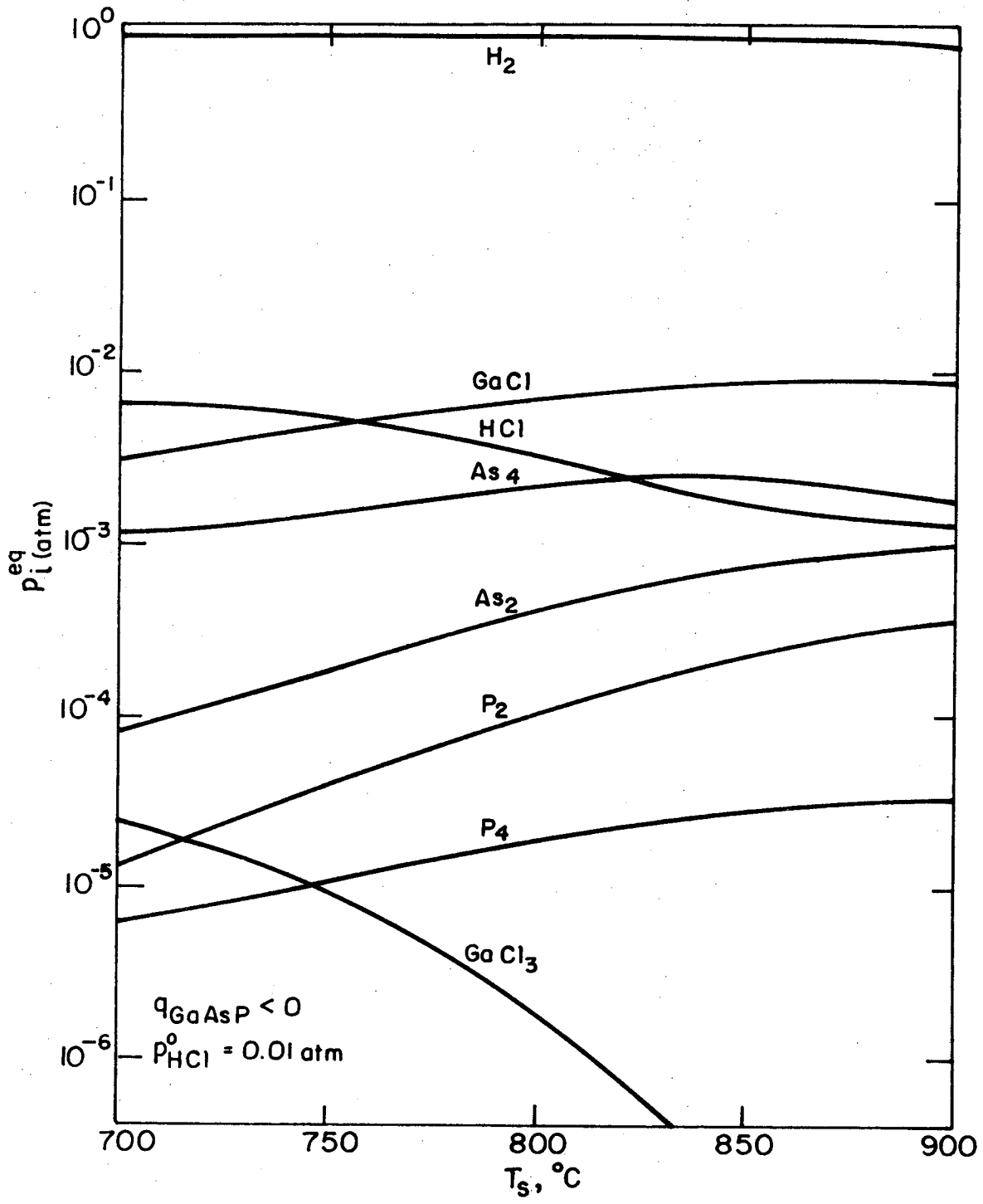
XBL 729-6987

Fig. 3a



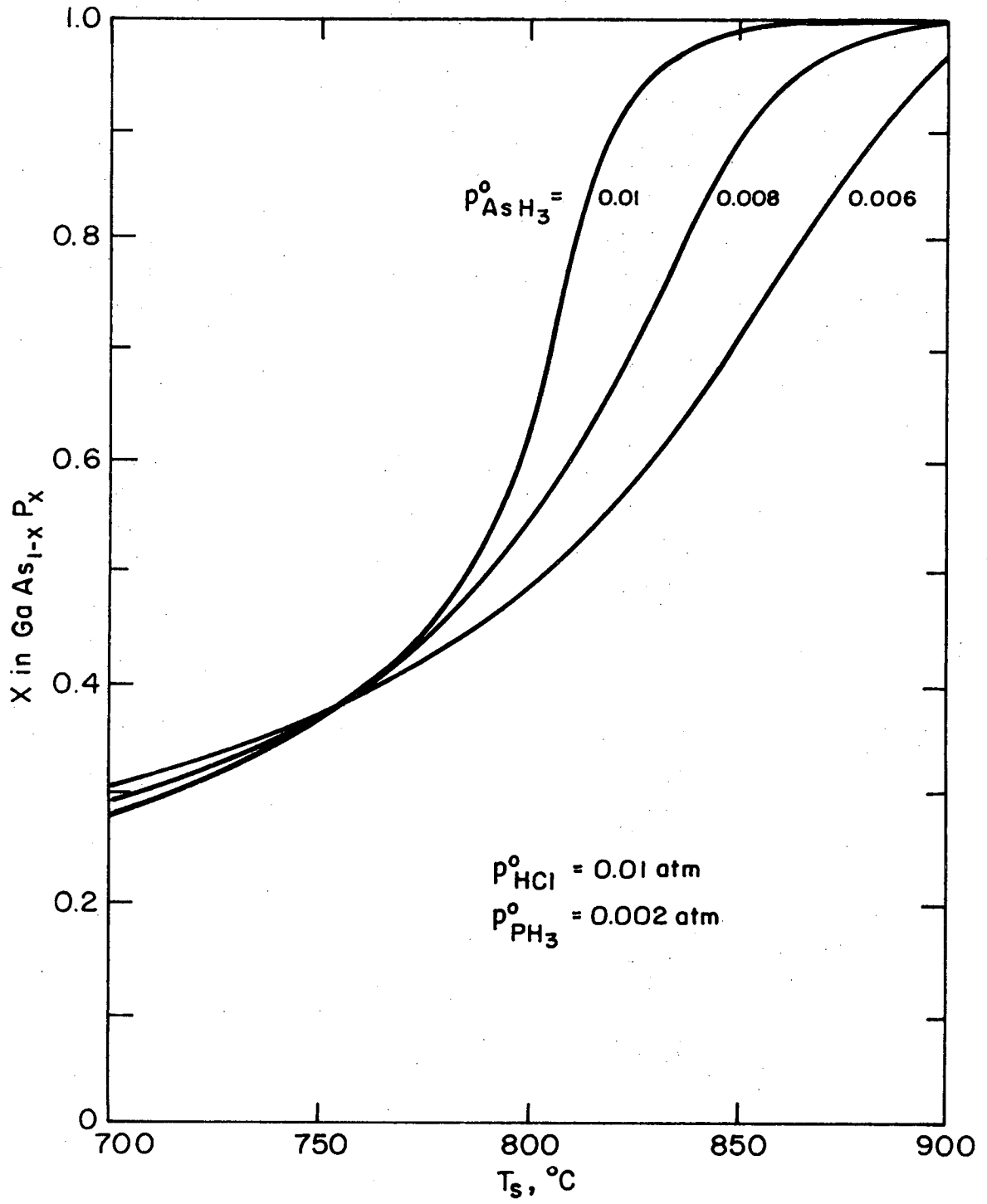
XBL729-6988

Fig. 3b



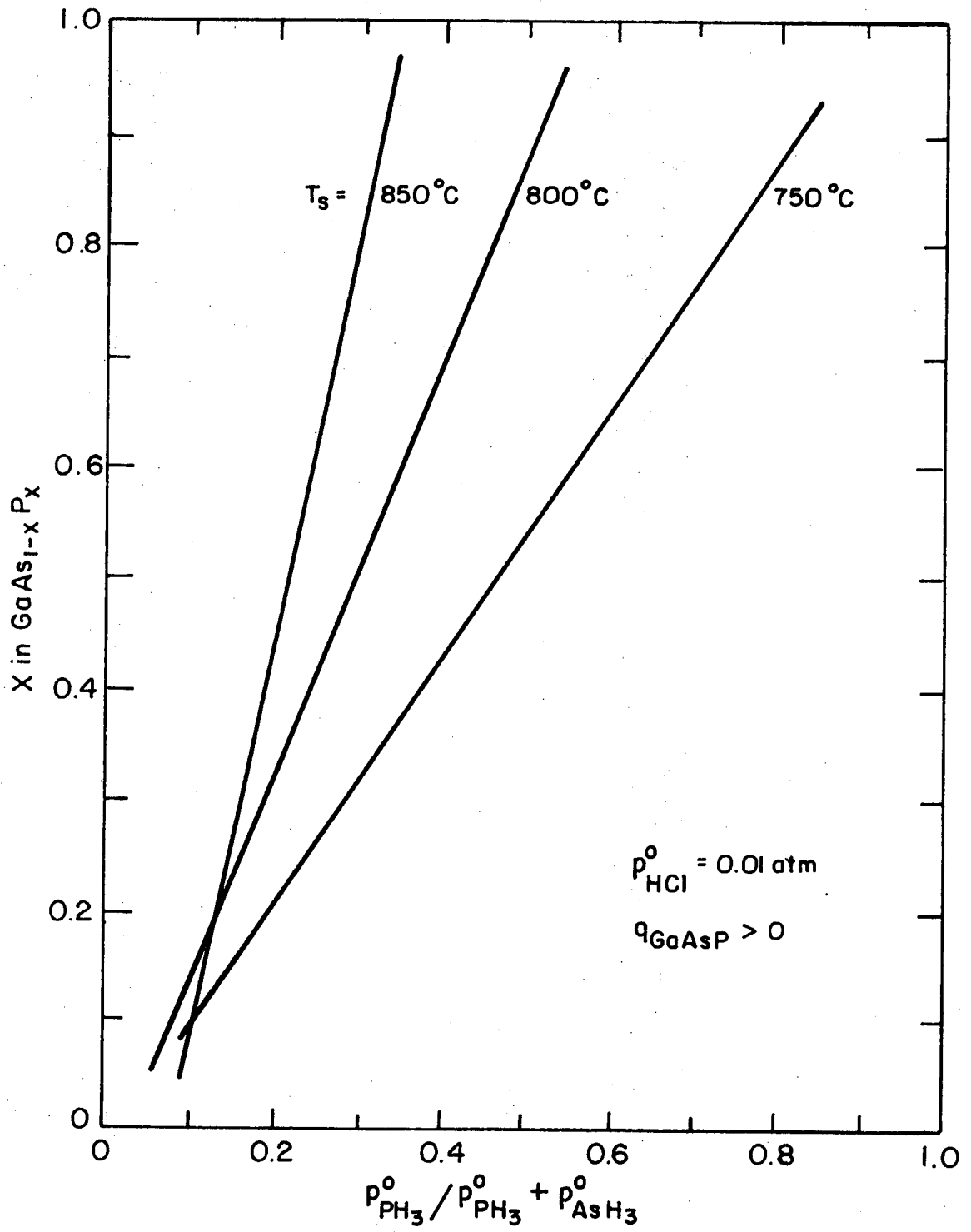
XBL729-6989

Fig. 3c



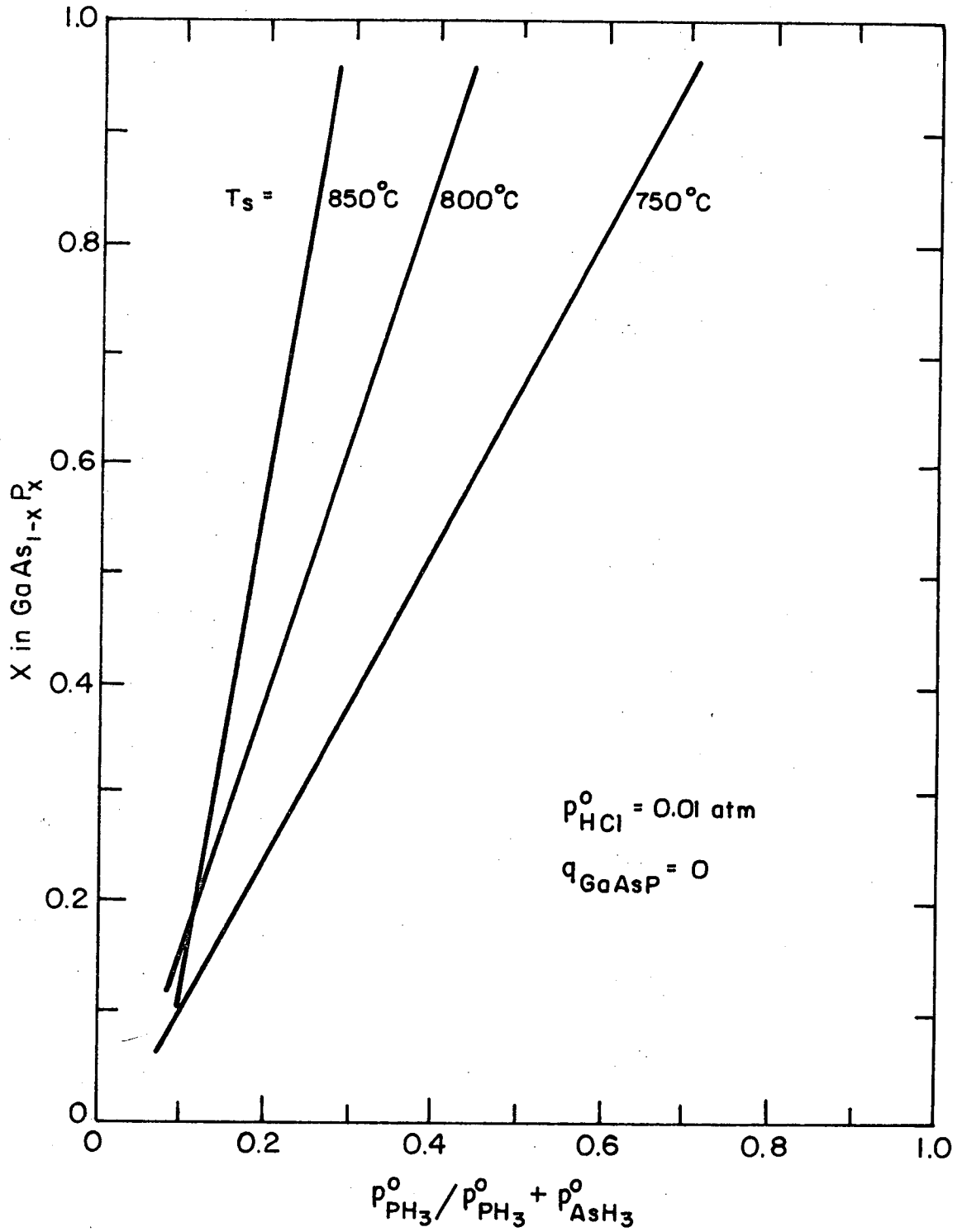
XBL 729-6 990

Fig. 4



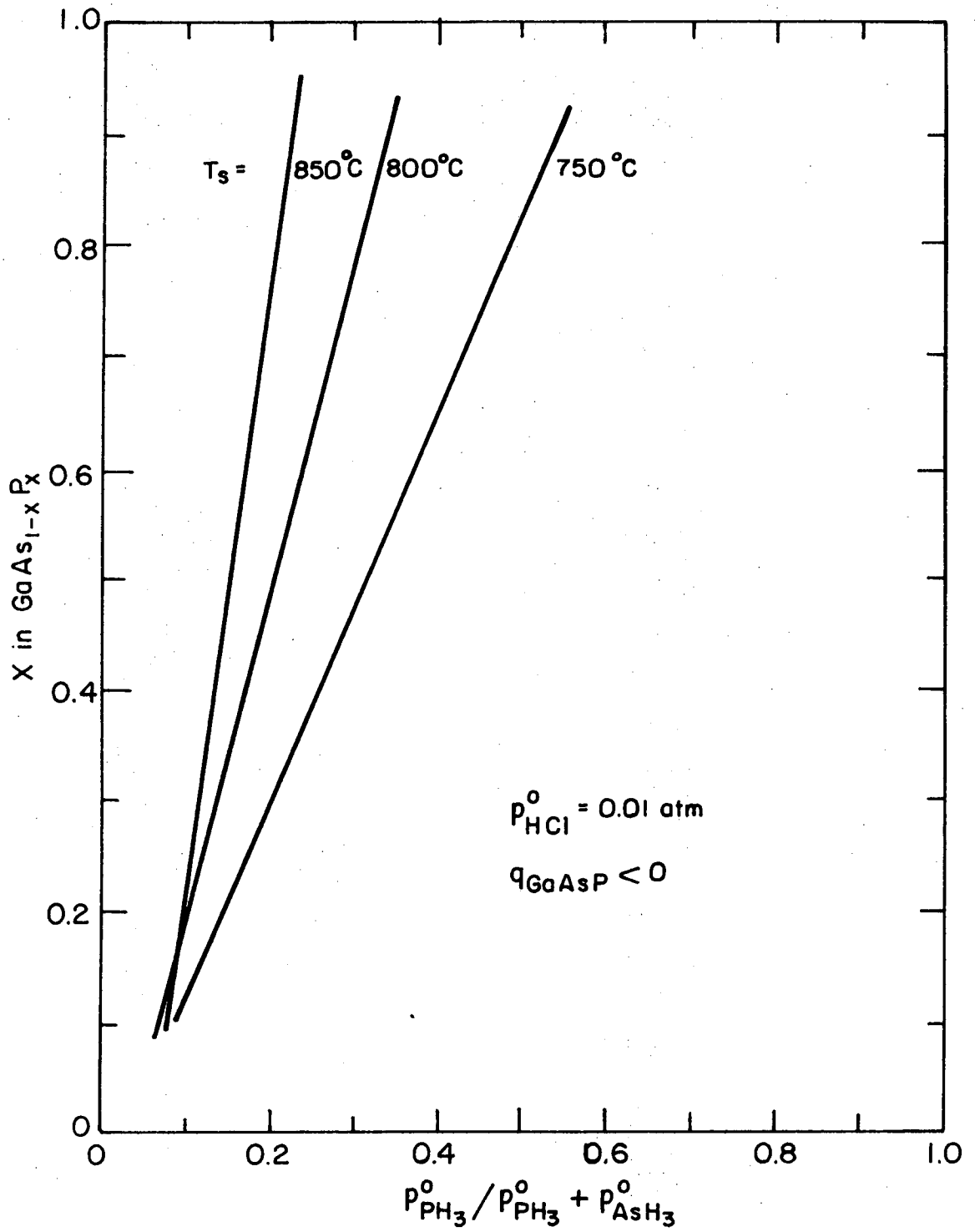
XBL 729-6991

Fig. 5a



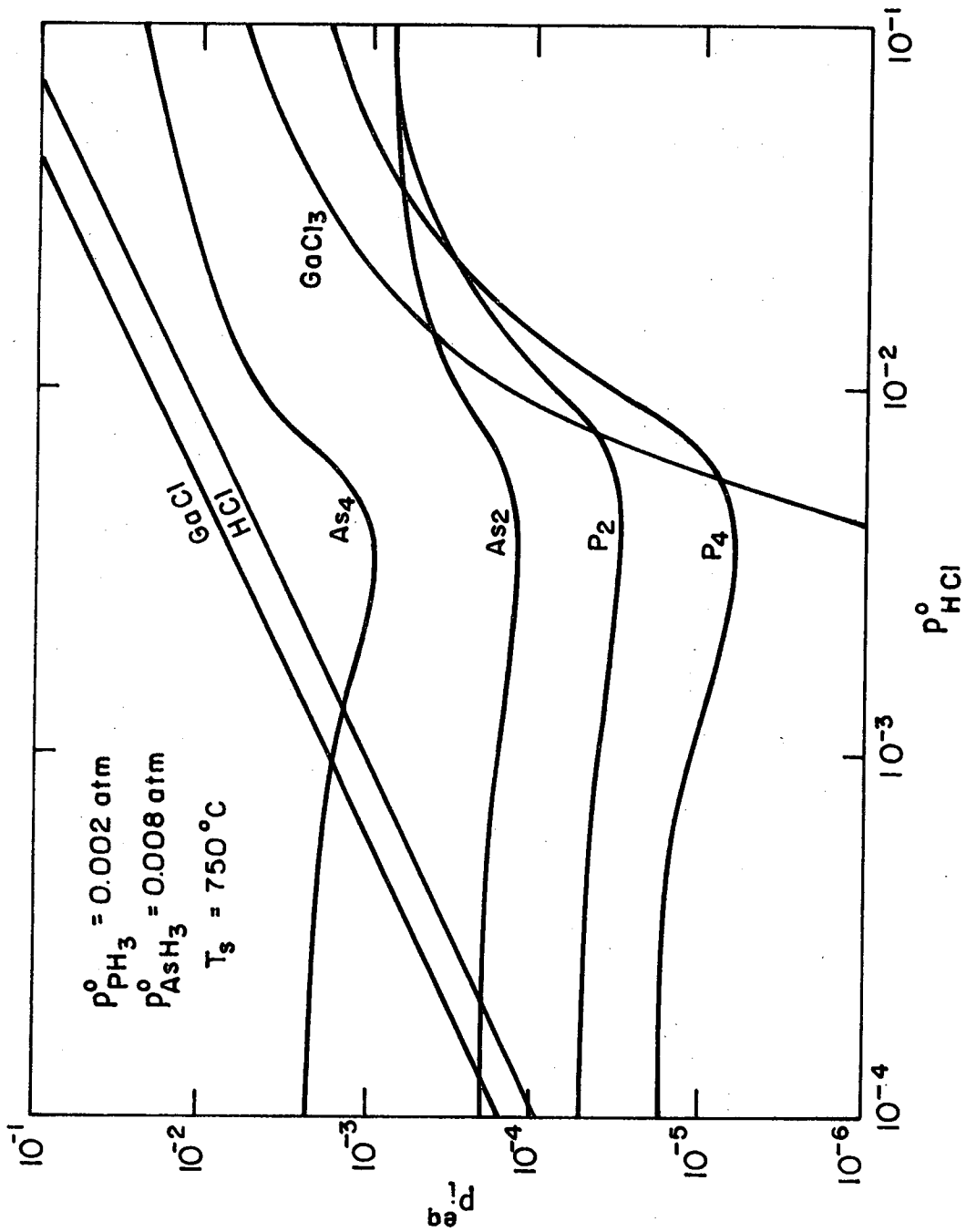
XBL 729-6992

Fig. 5b



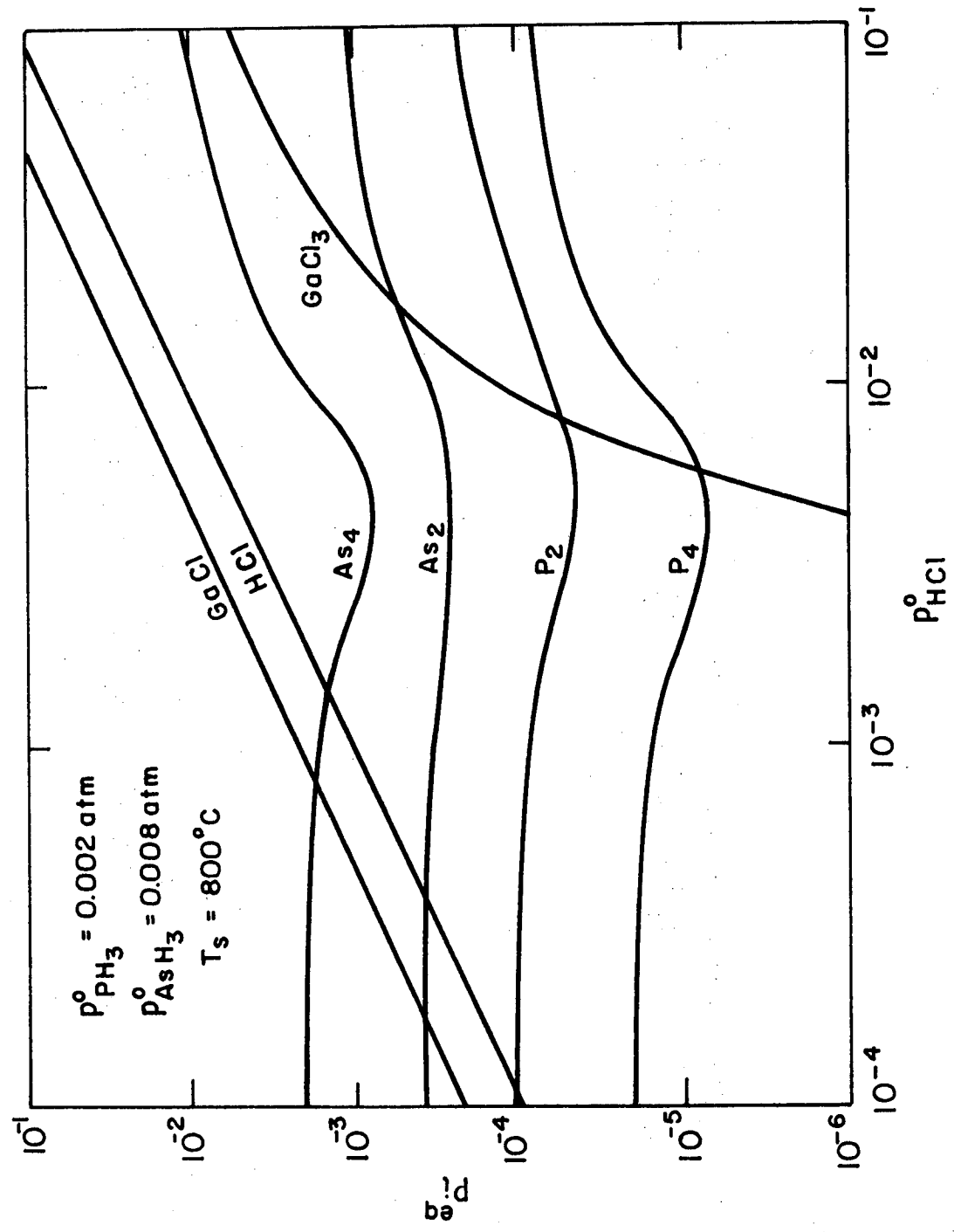
XBL729-6993

Fig. 5c



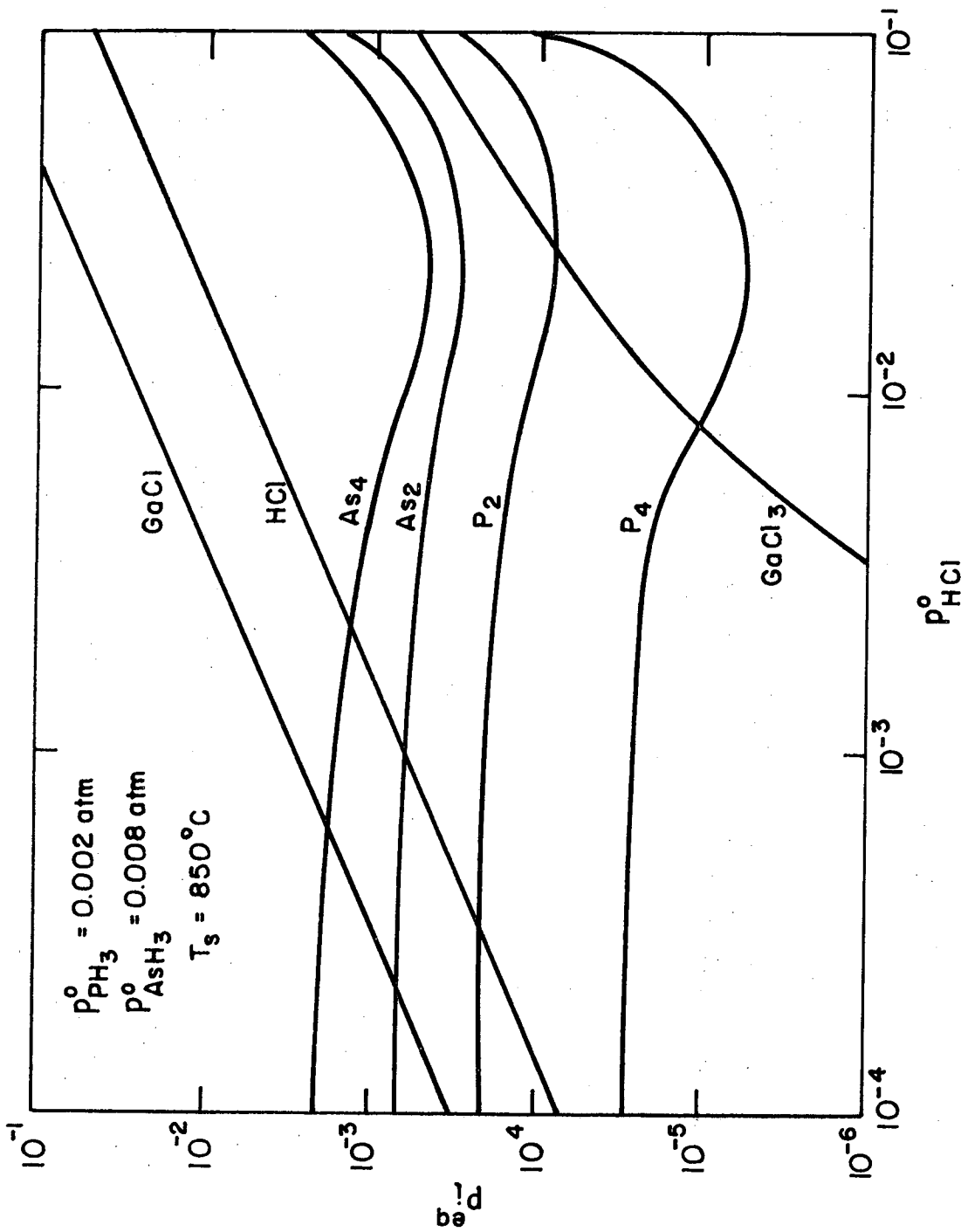
XBL 729-6994

Fig. 6 a



XBL 729-6995

Fig. 6b



XBL 729-6996

Fig. 6c

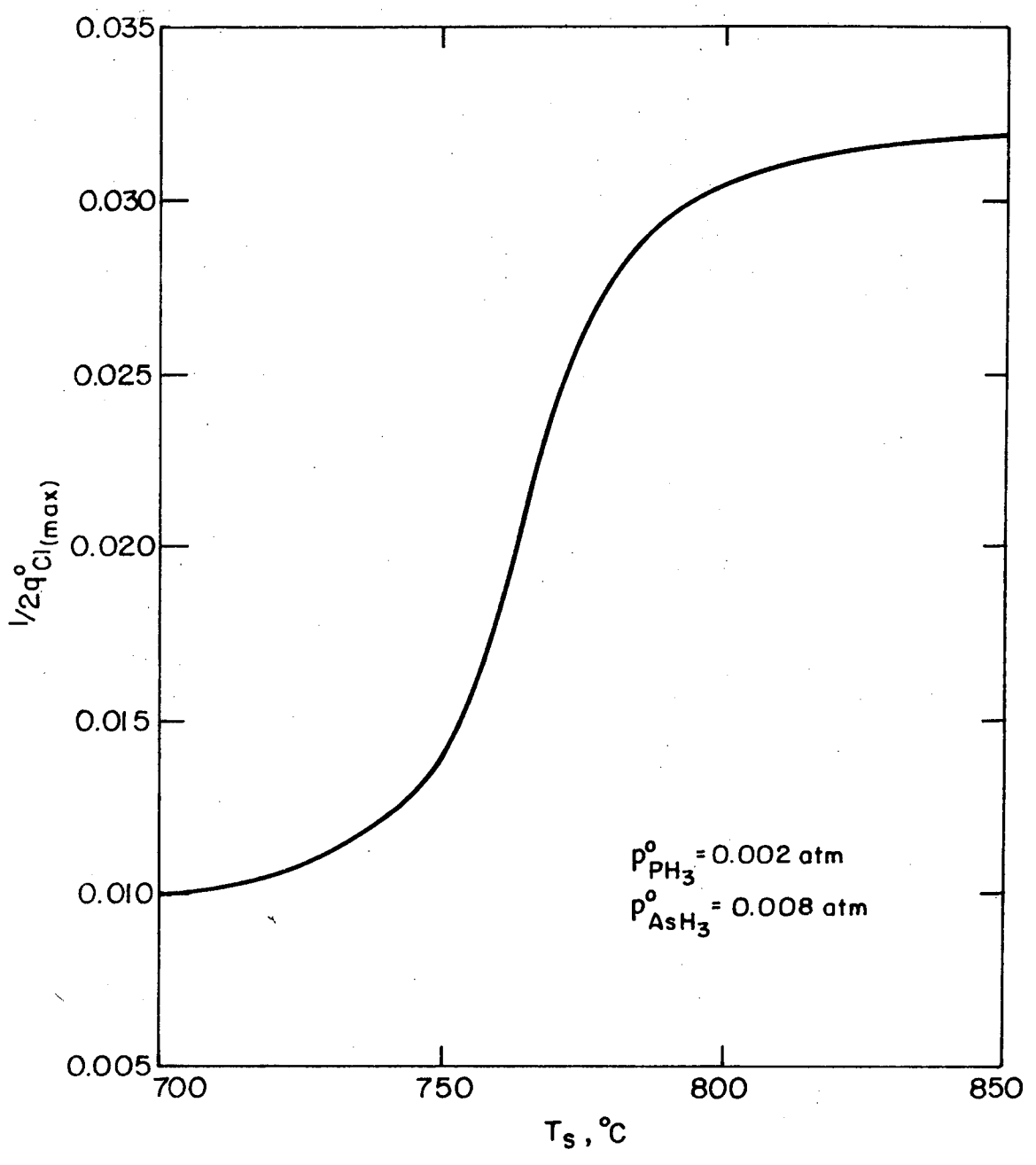


Fig. 7

XBL 729-6997

IV. DEPOSITION KINETICS

A. Introduction

The growth kinetics of $\text{GaAs}_{1-x}\text{P}_x$ from the gas phase system Ga-As-P-H-Cl is a complex process involving a large number of gaseous species and multiple reaction equilibria. Calculations of equilibrium either in the gas phase or at the gas-solid interface are insufficient to describe the deposition rate because the transport of reactants species to the solid, and product species away, requires a chemical potential gradient. Even when chemical equilibrium is assumed throughout the gas phase, the growth rate of the solid is controlled by the rates of diffusion through the gas, and by the reaction rates of adsorbed species on the surface to form the alloy solid.

Recent data by Shaw¹ indicates that the deposition reaction for GaAs is diffusion controlled for $T > 800^\circ\text{C}$. Shaeffer² also reports that surface reaction controlled growth by chemical transport becomes dominant only at temperatures below about 500°C . Since the group V elements As and P are expected to exhibit similar reactivity, the gas-solid deposition reaction for $\text{GaAs}_{1-x}\text{P}_x$ alloys is also expected to be at equilibrium at high temperatures. Consequently diffusion controlled kinetics should prevail in the temperature range from $800\text{--}900^\circ\text{C}$. Goettler³ has shown that the thermodynamics and mass transfer equations can be combined to allow calculation of the growth rate of GaAs, when the kinetics are diffusion controlled, or mixed diffusion and interface reaction controlled. In this section the basic principles of mass and heat transfer are applied to predict the deposition rates of $\text{GaAs}_{1-x}\text{P}_x$ resulting from the driving forces of concentrations of various gaseous species and temperatures.

B. Theory of Diffusion Limited Kinetics

For diffusion controlled kinetics the rate of solid phase deposition from the gas phase is governed by the diffusion of species to and away from the substrate within a laminar boundary layer with molar flux of the ith component toward the solid surface given by

$$N_i = CD_i \frac{d n_i/n_T}{dz}, \quad [\text{moles/cm}^2 \text{sec}] \quad (1)$$

when there is no fluid velocity normal to the substrate

where

C = molar density of the gas, $[\text{moles/cm}^3]$

D_i = gas phase diffusion coefficient for species i , $[\text{cm}^2/\text{sec}]$

n_i/n_T = molar fraction of species i

z = normal distance from the solid surface.

The mole fraction basis can be converted to partial pressure by the relation

$$\frac{p_i}{P} = \frac{n_i}{n_T} \quad (2)$$

for a gas of ideal behavior. For a fixed diffusion length δ the molar flux is simply

$$N_i = k_i \Delta p_i \quad (3)$$

where the mass transfer coefficient is

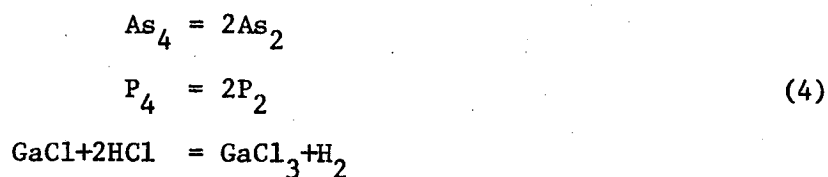
$$k_i = \frac{CD_i}{P\delta}$$

and

$$\Delta p_i = p_i' - p_i$$

is the difference between partial pressure outside the boundary layer, p_i' , and that at the solid surface, p_i .

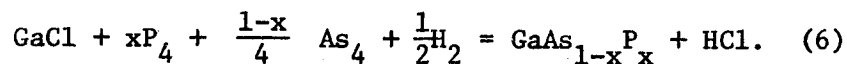
Since the gas phase diffusion and deposition reaction are assumed to be equilibrium processes, the equilibrium reactions described in Chapter III apply:



The molar flux equations for each component j must apply everywhere in the gas phase:

$$N_j = \sum_i \alpha_{ij} N_i = 0 \quad (5)$$

where the sum is taken over all species containing stoichiometric numbers α of component j . At the solid-liquid interface, however, Eqs. 4 apply in addition to the deposition reaction,



The molar flux Eqs. 5 apply for all components which do not appear in the $\text{GaAs}_{1-x}\text{P}_x$ product, i.e. H, Cl. The molar flux equations for Ga, As and P depend on the deposition rate however.

$$\begin{aligned} N_{\text{GaCl}} &= N_{\text{GaAs}_{1-x}\text{P}_x} \\ 4N_{\text{As}_4} &= (1-x)N_{\text{GaAs}_{1-x}\text{P}_x} \\ 4N_{\text{P}_4} &= xN_{\text{GaAs}_{1-x}\text{P}_x} \\ N_{\text{GaCl}} + N_{\text{HCl}} &= 0 \end{aligned} \quad (7)$$

Provided that the driving forces for the components Ga, As and P are in balance according to Eq. 7 the growth rate can be calculated from the molar flux of GaCl alone.

An example of the gas phase partial pressures within a laminar boundary is shown in Fig. 1. The well mixed gas is assumed to have a homogeneous composition outside the layer of thickness δ . The temperature change through a distance δ has an effect on the equilibrium constants, and should also be included in the calculations.

The precise calculation of the multicomponent diffusion-equilibrium problem is difficult in the general case. First, the properties of flow past the solid usually cause the diffusion length through the boundary layer, δ , to vary spatially. Also, the degree to which equilibrium is maintained should decrease with increasing gas flow rate. The equilibrium conditions in the gas phase and at the interface calculated in Chapter III can be used in the calculation of the deposition rate.

C. Boundary Layer Models

The properties of the deposition surface boundary layer, across which the gradients in component partial pressures are sustained, and consequently the diffusion length δ , depend on the direction of incident gas flow and on the geometry of the solid surface. Frequently encountered in epitaxial reactors are incident gas flows parallel, normal and at an oblique angle to the planar solid surface.

The gas phase composition can be most easily calculated within the surface boundary layer from boundary layer models. Three basic models are available which can be applied to this problem to describe properties of the boundary layer: 1) the film model, 2) the Leveque model, and 3) the laminar boundary layer model.

The film theory model assumes a uniform thickness of film formed by the flowing gases over the substrate. This theory is mainly used in systems where the flow is in turbulent regime. The mass transfer coefficient is given by the expression

$$k_i = \frac{CD_i}{P_\delta} \quad (8)$$

where δ is the thickness of the film. It is very difficult to estimate the value of δ . However, a precise knowledge of the process geometry can help to indicate its magnitude.

The Leveque boundary layer model assumes that the concentration varies linearly with distance normal to the surface. This assumption is applicable only in the laminar flow regime and no edge effects are taken into account when the flow is fully developed. The mass transfer coefficient is given by

$$k_C = 0.810 \left(\frac{CD_i}{P} \right)^{3/2} \cdot \left(\frac{a}{r} \right)^{1/3} \quad (9)$$

where a is a constant relating the change in flow velocity with distance and r is a length variable.

For the laminar boundary layer model, the gases velocity profile (or concentration profile) is parabolic over the solid surface. This theory can be applied to any system in which the flow is laminar, i.e. when the gases flow parallel to the substrate, normal to the substrate or when the substrate is rotating. The mass transfer coefficient is given by the expression

$$k_1 = 0.684 \left(\frac{CD_1 u_\infty^3}{P_v r_3} \right)^{1/6} \quad (10)$$

where u_∞ = bulk velocity of the gas
 ν = kinematic viscosity of the bulk of the gas
 r = distance along the surface from the edge, or disk center.

The average k_c can be found from this expression by integrating the expression from $r = 0$ to $r = r_0$. This model is applicable to the systems where the flow is in the laminar regime and is not fully developed, i.e. where edge effects are taken into account.

Schematics of the flow structures assumed for these three models are given in Fig. 2. Most of the $GaAs_{1-x}P_x$ deposition systems have very low flow rates because of the high costs of the starting gases. For silicoon deposition on the other hand, the flow rates are high and the deposition takes place with surface reaction limited kinetics at lower temperatures. For the $GaAs_{1-x}P_x$ reactor a laminar flow rather than a turbulent flow model is appropriate, whereas for silicon a turbulent flow model is best suited. Thus, for the present problem the film model allows a simplified calculation of the gas phase transport, but the laminar boundary layer model seems to be most appropriate to describe the gas flow properties.

D. Calculation of Deposition Rates

It was established above that the laminar boundary layer model is applicable to the deposition of $\text{GaAs}_{1-x}\text{P}_x$. In this section the growth rates are calculated based on the basic equation,

$$N_{\text{GaAs}_{1-x}\text{P}_x} = N_{\text{GaCl}} = k_{\text{GaCl}} \Delta p_{\text{GaCl}} \quad (11)$$

However, we need to correct this expression to take into consideration the change in gas temperature through the boundary layer since both k_{GaCl} and Δp_{GaCl} depend on the temperature drop across this layer. If k_{GaCl} is evaluated at the reaction zone temperature, then Eq. 11 can be written in the form,

$$N = k_{\text{GaCl}} \Delta p_{\text{GaCl}} \quad (\text{temperature correction term}) \quad (12)$$

Although it is very difficult to deduce the correction term, theoretically, it has been estimated empirically for various systems. For the deposition of $\text{GaAs}_{1-x}\text{P}_x$ (or GaAs, GaP) no data for any empirical correlation is yet available. However Kuznetsov⁴ has shown by a laminar boundary layer approach, that for chemical vapor deposition of silicon and germanium the correction factor for non-isothermal systems is $(T_s/T_g)^{-0.11}$ where subscripts g and s refer to reaction zone gas and solid respectively. He has also summarized exact relationships for calculation of deposition rates for various geometries (i.e., parallel flow, normal flow) using a laminar boundary layer model and basing his calculations on the similarity between mass, momentum and heat transfer (i.e., $\text{Pr} = \text{Sc} = \text{Le} = 1.0$) which is a very reasonable assumption for laminar flow. These relationships

require that a mass transfer parameter "b" appear instead of Δp_1 in Eq. 12. This parameter is

$$b = \frac{p^o - p^{eq}}{1 - p^{eq}} \quad (13)$$

and the deposition rate is

$$N_i = C \cdot u_\infty \cdot b \cdot S_T \cdot \left(\frac{T_{sub}}{T_{gas}} \right)^{-0.11} \quad (14)$$

Here S_T is the Stanton number, which for normal flow is

$$S_T = 0.47 \left(\frac{u_\infty x/2}{\nu} \right)^{1/2} \cdot P_r^{-2/3}$$

where $x/2$ = half width of the solid surface or substrate, i.e. radius of a disk substrate.

Equation 14 is basically the same as the one obtained by the simple laminar boundary layer model. The mass transfer parameter b can be simplified to Δp_{GaCl} as both p_1^{eq} and p_1^o are much less than unity, ($p_{eq}^i \approx 0.005$ atm). The expression for the growth rate is finally,

$$N_{GaAsP} (\text{gmoles/cm}^2\text{-sec}) = C u_\infty \Delta p_{GaCl} \left(\frac{T_{sub}}{T_g} \right)^{-0.11} S_T \quad (15)$$

From the above expression the deposition rates of $GaAs_{1-x}P_x$ can be easily estimated once the driving force and the flow properties of the system are known. A good initial approximation for physical properties of the gas phase is based on the fact that the gas is 98% hydrogen.

The deposition rate in gmoles $\text{cm}^2\text{-sec}$ can be converted to a linear rate, e.g. μ/min , for lattice parameter measurements for the alloy, which has been reported by Rubenstein⁵ and Pizzarello.⁶

E. Results and Discussion

The deposition rate of $\text{GaAs}_{1-x}\text{P}_x$ alloys was calculated from Eq. 15 for various temperatures of the substrate and a fixed temperature of the gases flowing to it. The calculated rates are functions of ΔP_{GaCl} and of $(\frac{T_S}{T_g})$, both of which depend on T_S . Results of the calculations are shown in Figs. 3 in which the value of N_{GaAsP} obtained for fixed initial conditions is plotted versus T_S . In Fig. 4 is shown the calculated growth rates in μ/min vs T for various input conditions for a constant $T_g = 900^\circ\text{C}$.

The results summarized in Figs. 3 and 4 show that the deposition rates decrease drastically with increase in the substrate temperature. This decrease can be expected because the gas temperature affects the driving force for the deposition process.

Figure 3 shows that there are three approximate regions for the deposition process. When $\frac{T_S}{T_g} \approx 0.88$, the growth rate curves show an inflection point. This probably is due to the fact that the temperature correction factor includes the effect of interface kinetics in the diffusion controlled regime well below 750°C . In the temperature interval from 750 to 850°C , the curves are almost linearly decreasing with temperature. Above 850°C the slope decreases rapidly.

Another result which can be deduced from Figs. 3 and 4 is that the growth rate does not depend significantly on q_{GaAsP} ; especially when

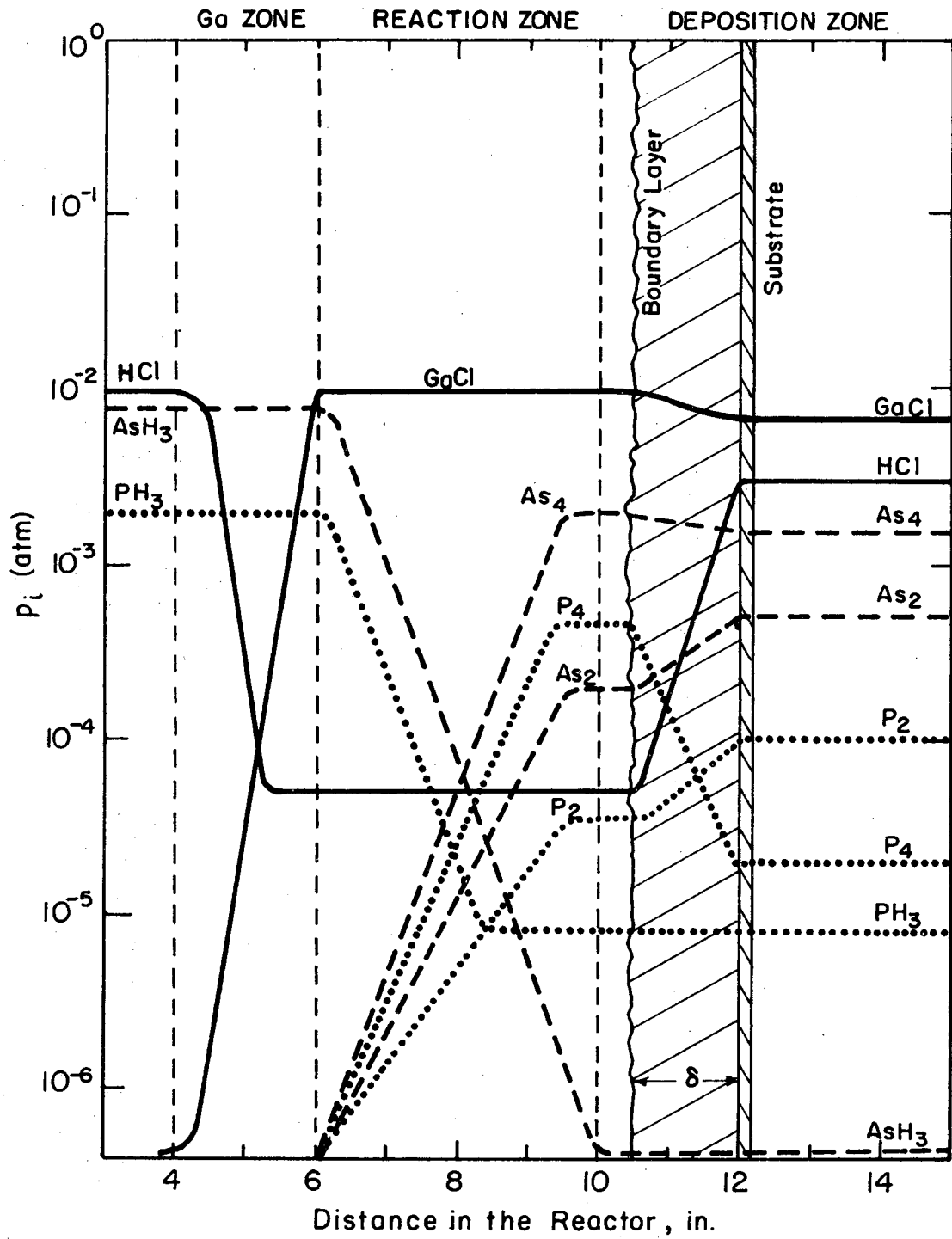
q_{GaAsP} is equal to or less than zero. The figures also show that growth rates are higher for positive q_{GaAsP} corresponding to an excess of GaCl. However, these plots do not give any indication for a maximum growth rate with decreasing substrate temperature, yet the maximum is expected since surface kinetic control dominates at low temperatures. Growth rates calculated by a different model by Goettler³ for GaAs also show that the growth rates increase when either partial pressure of GaCl or that of As_4 is increased over that in equilibrium with the substrate as expected. Goettler's experimental measurements of deposition kinetics for GaAs show, however, that a change in kinetics from diffusion control to interface reaction control occurs at about 750°C. A similar change should be expected for $\text{GaAs}_{1-x}\text{P}_x$ alloys, and the growth rate does not increase linearly with decreasing temperature, in agreement with the model on which Figs. 3 and 4 are based.

BIBLIOGRAPHY

1. D. W. Shaw, J. Electrochem. Soc. 115, 405 (1968).
2. H. Sheffer, Chemical Transport Reactions, (Academic Press, N. Y. 1964).
3. L. Goettler, "Diffusion and Surface Kinetics in the Epitaxial Vapor Deposition of GaAs" AIChE 67th National Meeting, February 1970.
4. F. A. Kuznetsov, J. Electrochem. Soc. 117, 785 (1970).
5. M. Rubenstein, J. Electrochem. Soc. 112, 426 (1965).
6. F. A. Pizzarello, J. Electrochem. Soc. 109, 226 (1962).

Figure Captions

- Fig. 1. Dependence of component partial pressures on position in $\text{GaAs}_{1-x}\text{P}_x$ reactor.
- Fig. 2. Boundary layer models for parallel, oblique and normal gas flow to a planar surface of finite length.
- Fig. 3. Dependence of growth rate of $\text{GaAs}_{1-x}\text{P}_x$ in $\text{gmoles/cm}^2\text{sec}$ on substrate temperature for different values of q_{GaAsP} .
- Fig. 4. Dependence of growth rate of $\text{GaAs}_{1-x}\text{P}_x$ in μ/min on substrate temperature for different values of q_{GaAsP} .



XBL729-7010

Fig. 1

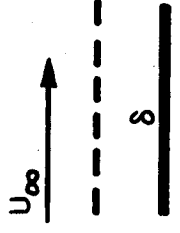
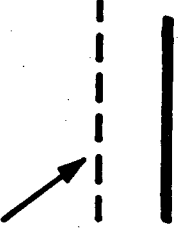
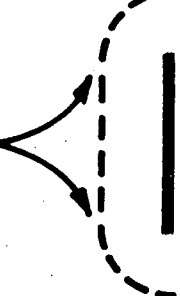
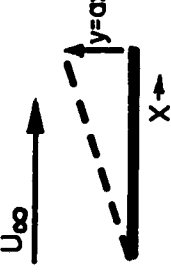
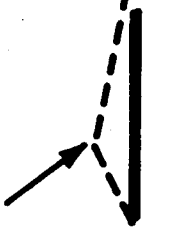
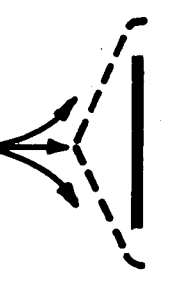
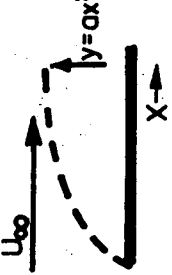
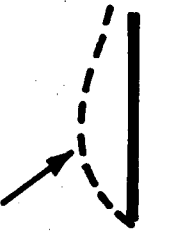

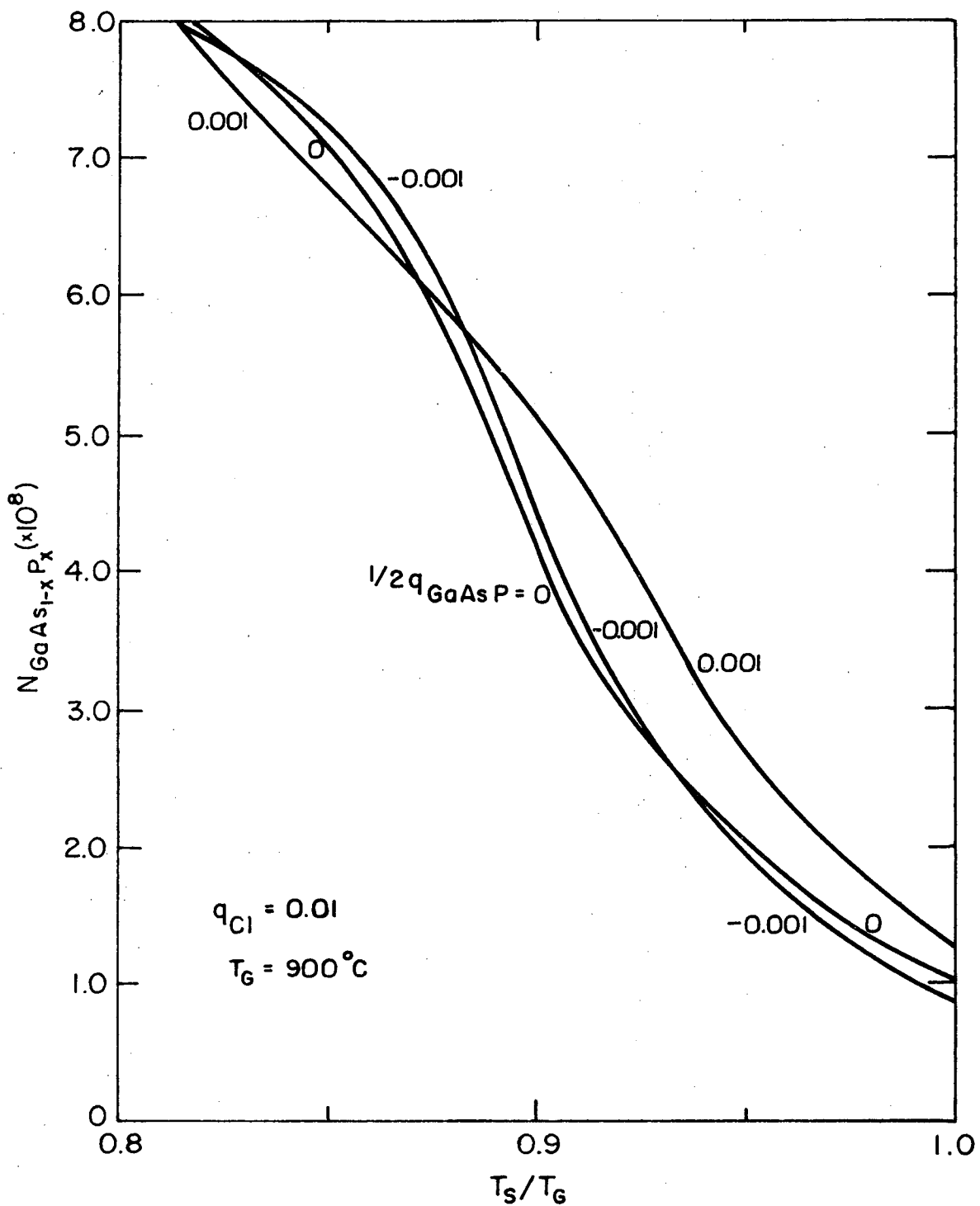
MODEL	PARALLEL FLOW	OBLIQUE FLOW	VERTICAL FLOW
FILM			
LEVÊQUE			
LAMINAR BOUNDARY LAYER			

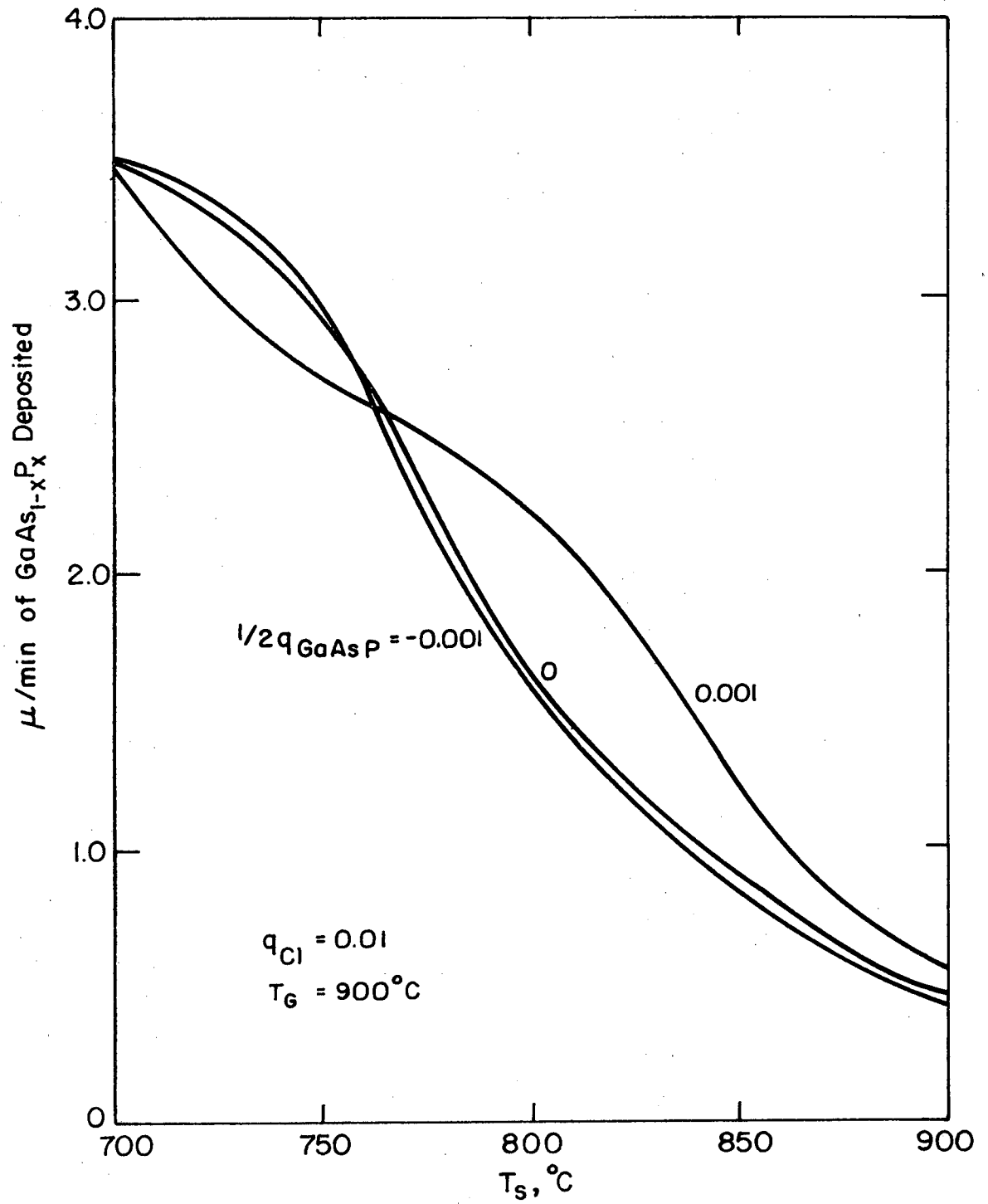
Fig. 2

XBL 729-6 998



XBL 729-6999

Fig. 3



XBL729=7000

Fig. 4

V. EXPERIMENTAL STUDY OF $\text{GaAs}_{1-x}\text{P}_x$ CHEMICAL VAPOR DEPOSITION

A. Introduction

An experimental study of the chemical vapor deposition process was undertaken to test the gas-solid equilibrium and to measure kinetic parameters from the deposition rates. The study encompassed the following steps: 1) design and construction of a reactor and gas flow system, and 2) operation of the system. These will be discussed in this chapter.

B. Reactor and Gas Flow System

A reactor was designed taking into consideration the conclusions reached in Chapter II. The reactor contained three zones. In the first gallium is contacted with incoming HCl to form GaCl. In the second, the reaction zone, gallium chloride, phosphorous and arsenic are mixed and reacted. In the third zone, called the deposition zone, deposition of $\text{GaAs}_{1-x}\text{P}_x$ (or GaAs, GaP) occurs over a substrate which is normal to the flow of the gases.

The overall reactor is shown schematically in Fig. 1. The reactor is made entirely of fused silica including the substrate holder.

In the gallium saturation zone, a 1/4 in. (6 mm) tube carries HCl in H_2 to the liquid gallium, contained in a 3 cm X 2 cm diameter crucible. The 1/4 in. tube is tapered at the end making a jet through which the gas enters a liquid gallium column about 2 cm high. The bubble size is approximately 1 mm dia. giving the HCl bubbles time to equilibrate with the gallium by forming gallium chloride. The reaction of gallium with HCl to form GaCl is virtually 100% at equilibrium.¹ A thermocouple well sits adjacent to the HCl input tube in the gallium crucible. The gallium

contactor is sealed to the reactor tube by a ground glass joint to facilitate loading and unloading of gallium.

Output gases from the gallium contactor pass through an orifice to mix with incoming arsine and phosphine in H_2 . The orifice prevents the flow of arsine and phosphine into the gallium saturator zone. A second orifice is provided at the middle of the reactor zone to thoroughly mix the gases by turbulent flow, and to thoroughly equilibrate the gases at the reaction temperature. The gases pass through a multi-orifice sieve plate at the end of the reaction zone; this creates a uniform velocity profile in the gases entering the deposition zone. The total length of the reaction zone is about 10 cm which is sufficient to give residence times of 2-5 sec for a typical 1 l/sec flow rate. The distance between the second orifice to the sieve plate is nearly 6 cm.

In the deposition zone, the substrate is held on the substrate holder with a thermocouple placed just below the substrate. The position of the substrate can be varied up and down in the reactor with the support rod secured by a Wilson seal. The maximum size of the substrate which can be placed on the substrate holder is 30 mm.

The effluent gases leave the reactor through a 1/4 in. tube below the substrate holder and pass through a trap containing a solution of KOH before entering a vent.

The reactor was heated by a Kanthal A wound three zone furnace with independent control of the temperature in each zone. A proportional controller and an on-off controller were used to control the temperature in the gallium zone and deposition zone respectively. The reaction zone temperature was unregulated. A typical temperature profile in the

furnace is shown in Fig. 2. The temperature gradient in the deposition zone required a correction of $+5^{\circ}\text{C}$ to the temperature of the thermocouple below the substrate. The temperature of the gallium crucible varied 15°C over its length but this does not affect the conversion of HCl to GaCl , as shown in Chapter III. Typical temperatures employed were 850°C for the gallium saturation, 900°C for reaction zone and 830°C for the substrate.

The flow system for gases is shown in Fig. 2. The gases used were of ultrahigh purity 99.999% or better, except for HCl which was of electronic grade. The gases, regulators values and flow meters, were obtained from the Matheson Co.

Argon was used as a purge gas. The gases were metered through high accuracy needle valves. Flows up to 2 ml/min were metered through Type 600 flow meters, and Type 602 meters were used for higher flow rates. Vacuum valves were used in the system wherever needed. All tubing to the reactor was 1/4 in. or 1/8 in. type 304 stainless steel. A 2 in. diffusion pumped vacuum system was used to initially purge the system, since it is essential for growth of good quality alloys that no impurities be present in the system.

C. Operation of the System

In a typical operation, the gallium saturator loaded with gallium and a substrate was placed on the substrate holder. Then the system was argon purged and evacuated. After the desired vacuum is reached (below 10 torr) the system is filled with hydrogen and heating is started. When the average temperature reaches about 700°C , the flows of arsine and phosphine are started at very low values (Goettler).² After the desired values of

temperature are reached, the flow of HCl is started with simultaneous increase in flows of AsH₃ and PH₃ and H₂. Typical flow rates are

$$\begin{aligned}R_{\text{HCl}} &= 10-15 \text{ cm}^3/\text{min, STP} \\R_{\text{AsH}_3} &= 8-10 \text{ cm}^3/\text{min, STP} \\R_{\text{PH}_3} &= 0-5 \text{ cm}^3/\text{min, STP} \\R_{\text{H}_2} &= 1000 \text{ cm}^3/\text{min, STP}\end{aligned}$$

After the deposition process had run for a desired period of time the furnace power and HCl flow were turned off, the AsH₃ and PH₃ flows reduced to very low levels and the H₂ flow decreased. The substrate was lowered into a cool zone to quench the sample. When the reactor temperature had fallen below 700°C the H₂ flow rate was further reduced and the AsH₃ and PH₃ flows stopped. The substrate was removed only after the reactor had cooled to room temperature and purged with argon to prevent oxidation of the gallium.

A sample calculation of the reactor conditions is produced in Appendix II. The complete partial pressure equilibria are obtained from the equilibrium data of Chapter III.

D. Results and Discussion

Extensive experimental data on CVD of GaAs_{1-x}P_x were not obtained due to initial difficulties in operating the system. Layers of GaAs, GaP and GaAs_{1-x}P_x were grown on both silicon and germanium substrates. [100] orientation, n-type silicon substrates were obtained from the Monsanto Co. These were lapped and polished by the supplier. Germanium wafers with [100] orientation were cut from single crystal germanium bars

grown from high purity Ge by the Czochralski method, then polished and etched in a 3:1:1 solution of HNO_3 , HF and HNO_3 (red fuming). The solution was boiled for five minutes with the wafer in it which resulted in etching. Only wafers with dislocations appeared etched.

Table I shows the results obtained in successful runs. As can be seen from it, usually polycrystalline growth took place due to the high density of nuclei on both Si and Ge substrates. It is known that Si is very susceptible to oxidation in the presence of oxygen and the oxide prevents epitaxy and increases the nuclei density tremendously. Ge, though less susceptible, is also oxidized by oxygen at high temperatures. This shows that the system was not clean enough and better procedure is required to purge the system to avoid the presence of oxygen. Another result of presence of oxygen (i.e. oxidation of Si to SiO_2) was that the deposited $\text{GaAs}_{1-x}\text{P}_x$ did not adhere to the surface of the substrate in spite of the little difference in their lattice parameters and coefficients of thermal expansion.

Another important result was that the experimental growth rates were much lower than the predicted ones. This could be due to many reasons. First, as pointed out earlier, due to the presence of oxygen the thermodynamic equilibria might have shifted. Secondly, it could be caused by the incomplete conversion of HCl to GaCl due to high flow rate of gases in the gallium container and hence not sufficient time for equilibration. Another reason can be the large kinetic barrier for growing GaAs, GaP and $\text{GaAs}_{1-x}\text{P}_x$ on Ge or Si.

There was less growth on the edges of the substrate than at the center. This was caused by the substrate holder wall. The wall is

higher than the substrate which causes the gases to flow over the edges without equilibrating with the substrate. This result supports the supposition that the flow is laminar over the substrate, as turbulence would promote uniform growth.

Characteristics of the $\text{GaAs}_{1-x}\text{P}_x$ deposits are shown in Figs. 3-5. In Fig. 3a is shown the results of GaAs deposited on a Ge substrate; the crystallite density is high and orientation appears partly random. The nucleation rate was probably very low since some of the crystallites have grown to larger size than have others. Most of the growing crystals have [100] orientation.

Figure 3b shows nuclei of GaP on a [100] and substrate, deposited under a very low driving force. The crystallites have [100] orientation.

$\text{GaAs}_{0.4}\text{P}_{0.6}$ was deposited on a Si substrate under a high driving force. Figure 4a shows that the growth of this composition was uniform, but the crystallites do not have a [100] orientation. Figure 4b shows the structure of a detached section of the deposit, as observed in a JEOL-1000 SEM. The height of various crystallites is more clearly seen here. Again the randomness appears in orientation of the grown crystallites. Figure 5a shows the edge effect caused by the substrate holder, showing the very little deposition taking place here as compared to that on the rest of the substrate. Figure 5b shows an enlarged view of one of the layer crystallites in the $\text{GaAs}_{0.4}\text{P}_{0.6}$ sample. The edges and boundaries are very clearly delineated. A very definite [111] orientation of the growth direction is evident.

The composition of the deposit in Exp. 11 was determined from the lattice parameter measured by x-ray diffraction using a Picker

diffractometer, and by assuming Vegard's law for the alloy. The measured composition $\text{GaAs}_{0.4}\text{P}_{0.6}$ with $x = 0.60 \pm 0.02$ agrees well with the theoretically predicted value of $x = 0.64$ obtained from Fig. 5c in Chapter III.

The measured growth rate for Exp. 11 with $0.35 \mu/\text{min}$. This corresponds to a molar flux of $\text{GaAs}_{0.4}\text{P}_{0.6}$ equal to 4.1×10^{-8} moles/min, whereas the theoretical molar flux based on the flux of gallium, N_{Ga} , was 9.3×10^{-8} moles/min. The ratio of experimental to theoretical growth rates for other experiments are shown in Table I. The low ratios for Exps. 6 and 9 indicate a low nucleation rate, and corresponding time lag before linear growth rates occur.

Table I

Experimental parameters and results in GaAs_{1-x}P_x growth.

Variable	Exp. 6	Exp. 9	Exp. 11
HCl flow, cc/min	10	10	10
AsH ₃ flow, cc/min	10	0	8
PH ₃ flow, cc/min	0	10	2
H ₂ flow with HCl, cc/min	500	500	500
H ₂ flow with AsH ₃ , PH ₃	500	500	500
Gallium saturator Temp (°C)	880	860	860
Reaction temperature	900	875	900
Substrate temperature	860	875	855
Deposition time (min)	30	30	60
Substrate	Ge	Si	Si

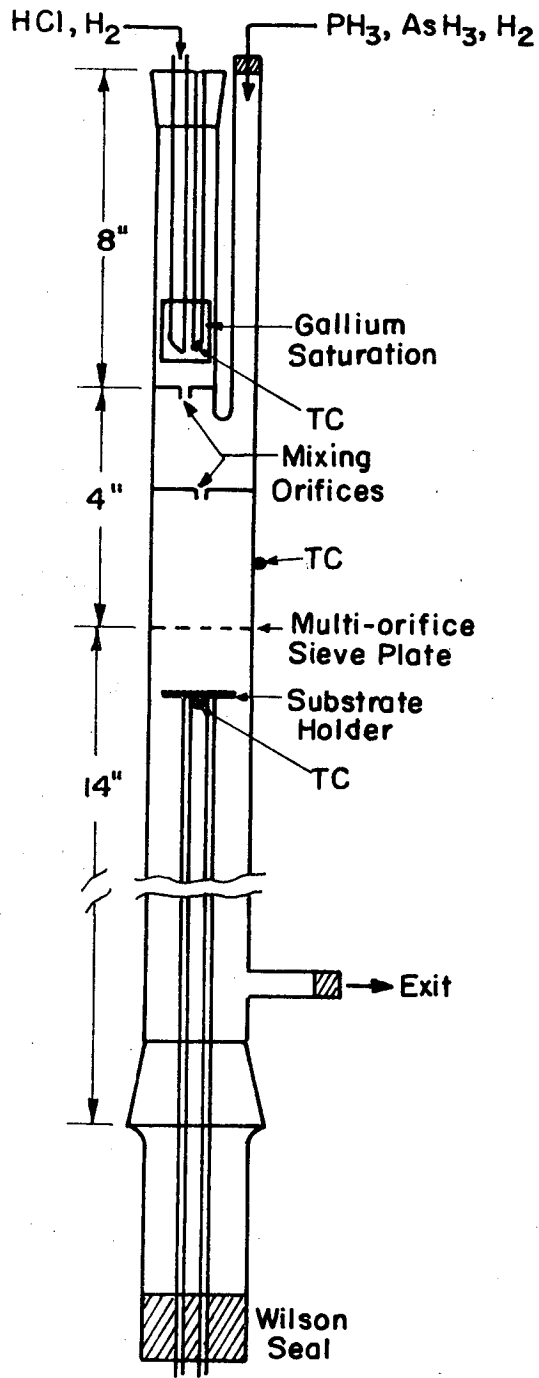
Results	Exp. 6	Exp. 9	Exp. 11
Type of growth	polycrystalline	nuclei only	polycrystalline
Growth rate (μ/min)	0.085	0.001	0.35
Composition, x	0	1.0	0.6
$N_{GaAsP}^{exp} / N_{GaAsP}^{theo}$	0.50	---	0.44
x_{exp} / x_{theo}	1	--	1.07

BIBLIOGRAPHY

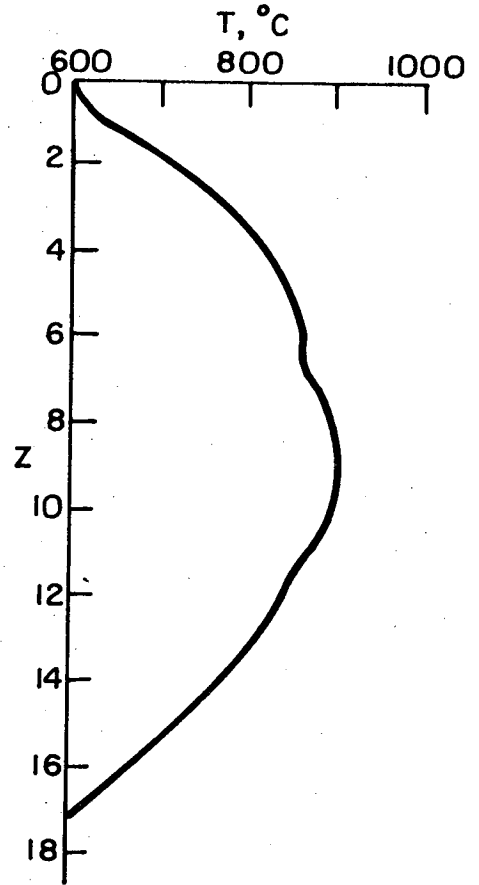
1. R. A. Ruherwein, "Manufacturing Methods for Growing GaAs, GaP Single Crystal Alloys" Contract no: AFML-TR-68-319, Monsanto Co. St. Louis, Mo., October 1968.
2. L. A. Goettler, "Diffusion and Surface Kinetics in the Epitaxial Vapor Deposition of GaAs," AIChE 67th National Meeting, Feb. 1970.

Figure Captions

- Fig. 1. Schematic of the experimental reactor for chemical vapor deposition of $\text{GaAs}_{1-x}\text{P}_x$ showing reactor cross section and temperature profile.
- Fig. 2. Schematic of the gas feed system for the $\text{GaAs}_{1-x}\text{P}_x$ reactor.
- Fig. 3. Nucleation of GaAs and GaP.
 - a. GaAs on a [100] Ge substrate ($\times 1000$)
 - b. GaP on a [100] Si substrate ($\times 1000$)
- Fig. 4. a. Polycrystalline growth of $\text{GaAs}_{0.4}\text{P}_{0.6}$ on a [100] Si substrate under high growth rate conditions ($\times 160$).
 - b. Oblique view of polycrystalline $\text{GaAs}_{0.4}\text{P}_{0.6}$ deposited on [100] Si after detachment and fracture ($\times 1000$).
- Fig. 5. a. Edge effect due to the substrate holder on deposition rate.
 - b. Preferred growth of $\text{GaAs}_{0.4}\text{P}_{0.6}$ showing surface structure for growth in $\langle 111 \rangle$ direction.



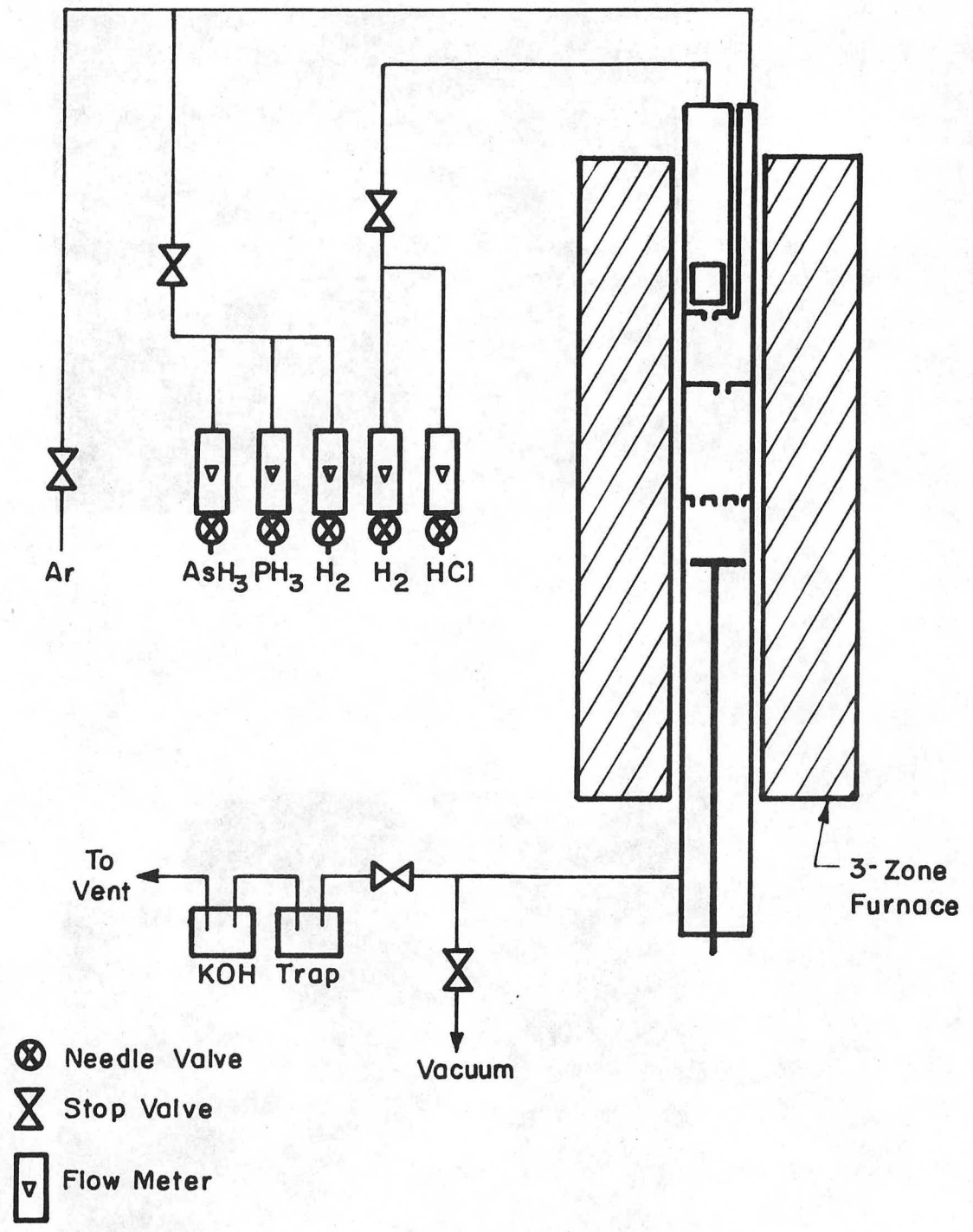
(a) Reactor Cross-section



(b) Temperature Profile

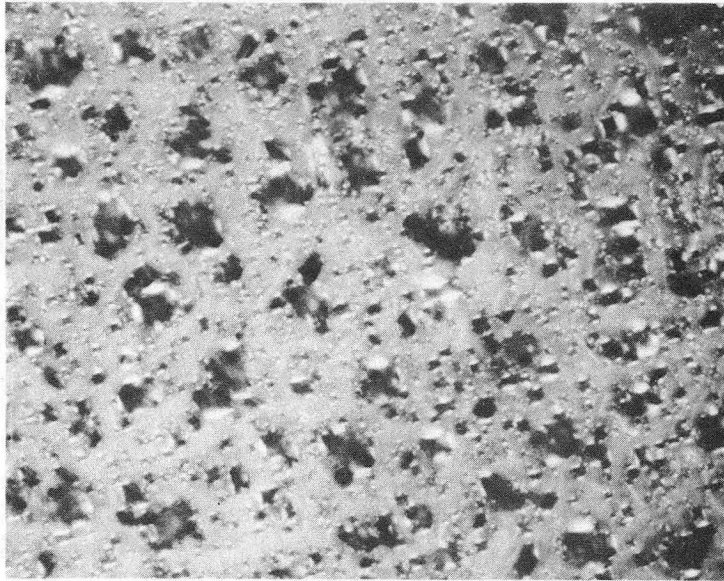
XBL729-7001

Fig. 1

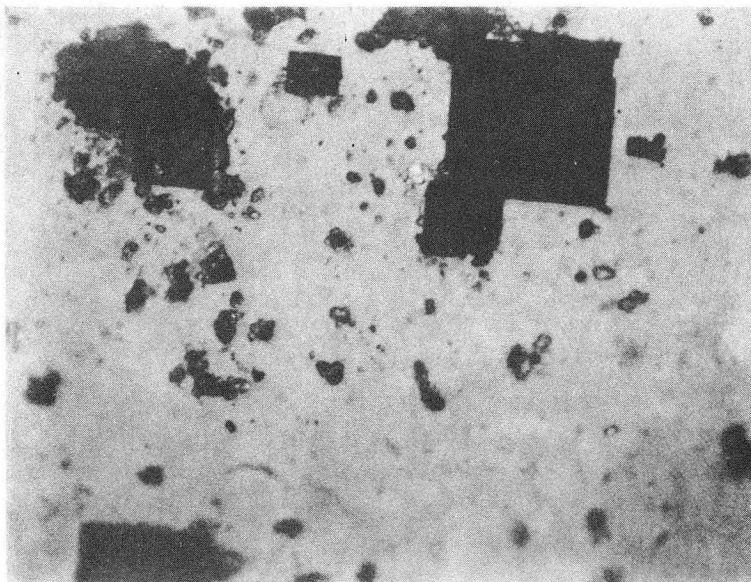


XBL 729-7002

Fig. 2



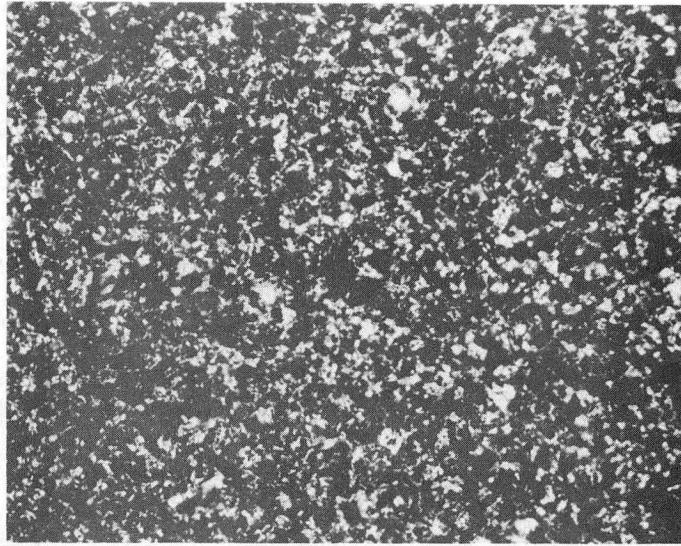
(a)



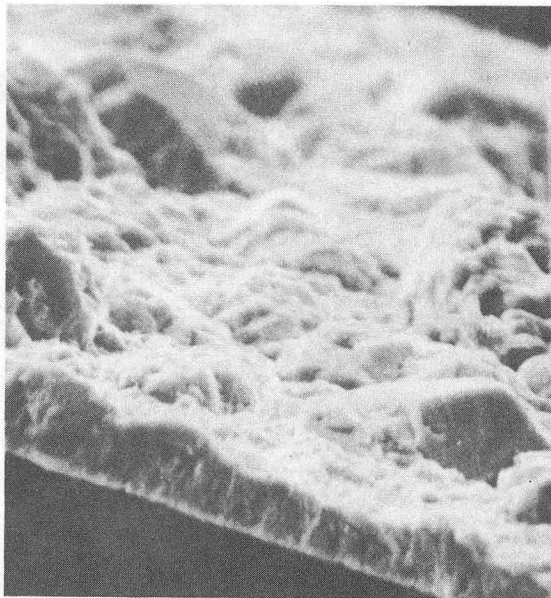
XBB 729-4854

(b)

Fig. 3



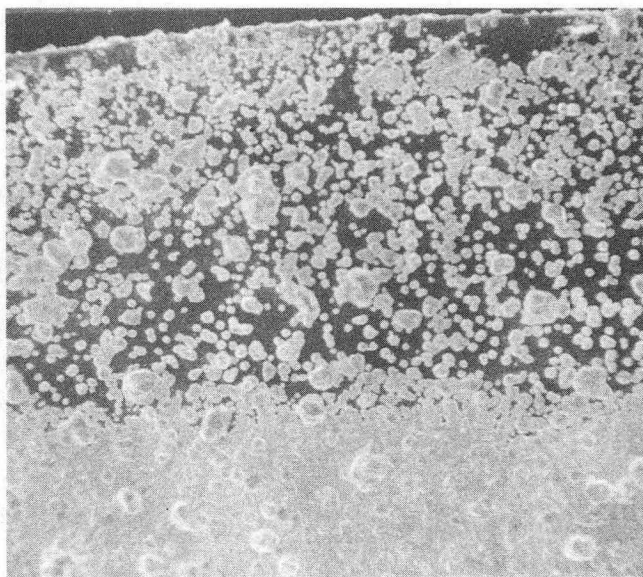
(a)



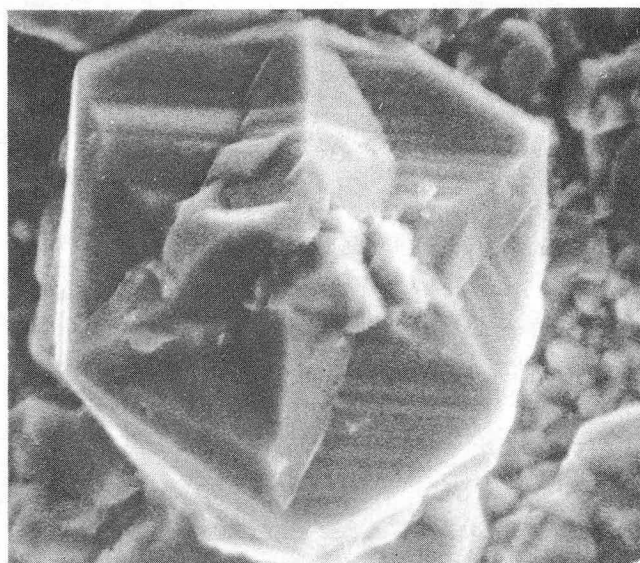
XBB 729-4853

(b)

Fig. 4



(a)



XBB 729-4855

(b)

Fig. 5

VI. CONCLUSIONS

The process of chemical vapor deposition of $\text{GaAs}_{1-4}\text{P}_x$ from $\text{Ga}(\ell)$, PH_3 , AsH_3 , HCl and H_2 source materials requires detailed information on the thermodynamics of phase equilibria and deposition kinetics, as well as appropriate design of the reactor to obtain maximum efficiency and control of the product phase. From the present study the following conclusions are drawn.

1. Many source materials are possible, e.g. solid As, liquid chlorides of phosphorous and arsenic etc., but the most convenient for industrial application are gaseous reactants, and particularly those containing the transport agent, i.e. hydrides. But $\text{Ga}(\ell)$, as a reactant, is an exception because no stable compound of gallium is a gas at room temperature and one atmosphere which is also available in a pure form.
2. The gallium saturator should operate at equilibrium in order to allow prediction of the gas phase composition correctly.
3. Mixing of the gases is needed in the reaction zone in order to homogenize the gas phase, thereby providing a uniform composition at the growing surface.
4. Laminar flow of reactant gases over the substrate is desirable, as is a high residence time for contact between solid and gas to insure complete reaction to equilibrium.
5. There is a need to prevent oxygen contamination in the reactor since it reacts violently with PH_3 , and acts as an electrically active dopant in $\text{GaAs}_{1-x}\text{P}_x$. It shifts the thermodynamic equilibria which results in a wrong prediction of equilibrium properties and growth rates. Oxygen also attacks the substrate and due to its oxidation, no epitaxial growth is possible.

6. The P/P+As ratio in the gas phase was found from calculations to be lower than that in the solid which is in equilibrium with the gas.

7. Experimental determination of x is in good agreement with our theory which includes the effect of a finite growth rate.

8. An excess of GaCl over the stoichiometric amount is required for the most efficient utilization of the group V reactants. The GaCl partial pressure required for maximum efficiency increases with temperature.

9. Polymers of arsenic and phosphorous should be included in the equilibrium calculations since their concentration is 10-20% of the total arsenic and phosphorous present. Experimental measurements of the reaction equilibrium constants for these compounds are needed.

10. There is a need to keep the reaction zone temperature higher than the temperature at which $\text{GaAs}_{1-x}\text{P}_x$ is in equilibrium with the gas in the reaction zone, otherwise deposits will take place on the walls of the reactor.

11. The growth rate increases with decreasing substrate temperature for a fixed input gas. For diffusion controlled kinetics, the rate of change of growth rate goes through a maximum with decreasing temperature.

12. Experimentally measured growth rates are lower than expected from theory. This is caused by a) presence of oxygen which shifts the thermodynamic equilibria, b) a large kinetic barrier for nucleating $\text{GaAs}_{1-x}\text{P}_x$ and GaP on silicon and GaAs on germanium.

The following further studies are needed for a better understanding of this system.

1. The effect of HCl excess in the gas phase over on deposition efficiency and phase equilibria.

2. The effect of temperature driving force and interactions of the concentration driving forces for various gaseous species on the deposition rates.

3. The effect of group V polymer on the thermodynamic behavior of the system.

ACKNOWLEDGEMENTS

I am very grateful to Dr. L. F. Donaghey for his constant encouragement, guidance and constructive criticism without which this work would not have been possible. Thanks also go to Dr. R. L. Pigford and Dr. W. G. Oldham for their comments and suggestions which helped in preparing the final manuscript.

Thanks also to Mr. Bill Hart for building the reactor, Mr. Brian Pope for building the furnace and Mr. Phillip Eggers for his help in using the electronic equipment.

My special thanks to Mrs. Shirley Ashley, who was burdened with typing and Mrs. Gloria Pelatowski who did the drawings.

This work was done under the auspices of the U. S. Atomic Energy Commission.

APPENDIX I

Sample Calculations of Thermodynamics of Phase Equilibria
in the Ga-As-P-Cl-H System

A. Gallium Saturation Equilibria

For solving the gallium saturation equilibria Eq. 20 of Chapter III was derived. At a temperature of 850°C the relevant equilibrium constants are $k_1 = 10^{6.45}$, $k_2 = 10^{16.88}$ and $k_5 = 10^{4.67}$. Coefficients in Eq. 20 are then

$$C_1 = (1 + k_5/k_1)/3(k_2/k_1^3) = 100$$

and

$$C_2 = \frac{1}{3(k_2/k_1^3)} = 99$$

Equation 20 then reads,

$$P_{\text{GaCl}}^3 + 100 P_{\text{GaCl}} - 99 q_{\text{Cl}}^\circ = 0.$$

By iterative solution we obtain $P_{\text{GaCl}} = 0.995 q_{\text{Cl}}^\circ$. Equations 17 and 18 now can be solved for P_{HCl} and P_{GaCl_3} respectively.

When

$$q_{\text{Cl}}^\circ = 0.01, \text{ the partial pressures in the system are}$$

$$P_{\text{HCl}} \approx 0.01 \text{ atm.}$$

$$P_{\text{HCl}} \approx 0.00005 \text{ atm.}$$

and

$$P_{\text{GaCl}_3} \approx 10^{-8} \text{ atm.}$$

B. Reaction Zone Equilibria

The arsenic equilibria, using Eq. 32 in Chapter III, can be solved. At 850°C ($K_7 = 10^{-3.63}$, $K_8 = 10^{-9.46}$). Then for $q_{As} = 0.01$, Eq. 32 becomes

$$p_{PAs_4} + 0.0038 p_{As_4}^{1/2} + 8.65 \times 10^{-10} p_{As_4}^{1/4} - 0.0025 = 0.$$

Neglecting the term containing the coefficient 10^{-10} we obtain the iterative solution $p_{As_4} = 0.0023$ atm.

Then, from Eqs. 23 and 25 in Chapter III p_{AsH_3} and p_{As_2} are $\sim 10^{-10}$ atm and 0.000366 atm respectively.

Phosphorous equilibria can then be calculated using Eq. 32 at 850°C with $q_p = 0.01$, where $k_{14} = 10^{-2.79}$ and $k_{15} = 10^{-2.24}$. Consequently, Eq. 32 becomes

$$p_{P_4} + 0.0199 p_{P_4}^{1/2} + 0.00144 p_{P_4}^{1/4} - 0.0025 = 0.$$

Solving again by iteration, we find

$$p_{P_4} = 0.00164 \text{ atm.}$$

Substituting this value in Eqs. 24 and 26 we then find that p_{PH_3} and p_{P_2} are 0.000056 atm and 0.00029 atm respectively.

C. Deposition Zone Equilibria

Deposition zone equilibria can be solved by using Eq. 51 of Chapter III. Assume $T = 800^\circ\text{C}$, and $p_{HCl}^\circ = 0.01$, $p_{PH_3}^\circ = 0.002$ and $p_{AsH_3}^\circ = 0.008$ atm. Then for $q_{Cl} = 0.01$, $q_{GaAsP} = 0$ and $q_p/q_{As} + q_p = 0.2$, we find, $A = 4.0165$ and $B = 0.0222$. So, Eq. 51 becomes

$$p_{GaCl} \left[\pm \left(4.018 p_{GaCl}^{1/2} - 0.0222 \right)^{1/2} \right] + 1.18 p_{GaCl}^{-0.0118} = 0$$

Successive approximation, then gives the solution

$$P_{\text{GaCl}} = 0.0068 \text{ atm}$$

The remaining species, P_{HCl} , p_{As_4} , p_{As_2} , p_{P_4} and p_{P_2} are obtained by substituting P_{GaCl} into Eqs. 40, 50, 36, 38, 39, and 35, respectively.

These equations give

$$P_{\text{HCl}} = 0.0031 \text{ atm}$$

$$p_{\text{As}_4} = 0.00150 \text{ atm}$$

$$p_{\text{As}_2} = 0.000345 \text{ atm}$$

$$p_{\text{P}_4} = 0.0000136 \text{ atm}$$

$$p_{\text{P}_2} = 0.000070 \text{ atm}$$

Finally, by material balance of arsenic and phosphorous it is found that

$$x = \frac{\Delta p_{\text{P}}}{\Delta p_{\text{P}} + \Delta p_{\text{As}}} = 0.581$$

APPENDIX II

Sample Calculations for Growth Rate Prediction Experiment 11

The conditions of Exp. 11 are used in the following calculations.

Flow rate of HCl during the experiment = 10 cc/min and $p_{\text{HCl}}^{\circ} = 0.01$ atm.

Flow rate of AsH₃ during the experiment = 8 cc/min and $p_{\text{AsH}_3}^{\circ} = 0.008$ atm.

Flow rate of PH₃ during the experiment = 2 cc/min and $p_{\text{PH}_3}^{\circ} = 0.002$ atm.

Flow rate of H₂ during the experiment = 1000 cc/min and $p_{\text{H}_2}^{\circ} = 1.0$ atm.

The average temperature of the substrate during the experiment = 854°C.

The average temperature of the gallium saturator during the experiment = 862°C

The average temperature of the reaction zone during the experiment = 920°C.

The mass constraints are $q_{\text{Cl}} = 0.011$, $q_{\text{As}} = 0.008$, $q_{\text{P}} = 0.002$ and $q_{\text{GaAsP}} = 0$.

The equilibrium partial pressures of all the gaseous species over the substrate can be read from Fig. 3(b), Chapter III.

i.e.

$$p_{\text{GaCl}} = 0.0084 \text{ atm}$$

$$p_{\text{HCl}} = 0.0016 \text{ atm}$$

$$p_{\text{As}_4} = 0.0016 \text{ atm}$$

$$p_{\text{As}_2} = 0.00062 \text{ atm}$$

$$p_{\text{P}_4} = 0.000021 \text{ atm}$$

$$p_{\text{P}_2} = 0.00019 \text{ atm}$$

The expected compound to be formed is GaAs_{0.305}P_{0.695}. The pressure driving force for deposition, Δp_{GaCl} is 0.0016 atm. Equation 15 of Chapter IV can be used to predict the growth rate in gmol/cm²-sec.

For laminar flow $Pr = 1.0$ and the correction coefficient containing Pr is unity. The temperature of bulk of the gas is nearly 900°C and u_∞ , C and at this temperature are

$$u_\infty = \frac{\text{total flow rate}}{\text{cross section area of the reactor}} = 1.5 \text{ cm/sec.}$$

$$C = 1.12 \times 10^{-5} \text{ gmoles/cm}^3$$

$$u_\infty = 0.99 \mu_{\text{H}_2} + 0.01 \mu_{\text{GaCl}} = 9.04 \times 10^{-5} \text{ gmoles/cm-sec}$$

$$L/2 = \text{radius of the substrate} = 1.575 \text{ cm.}$$

The molar flux equation is then

$$N_{\text{GaAs}_{1-x}\text{P}_x} = 4.15 \times 10^{-6} \times \Delta p_{\text{GaCl}} \times \left(\frac{T_{\text{sub}}}{T_g} \right)^{-0.11}$$

For $T_{\text{sub}} = 850^\circ\text{C}$, $T_g = 900^\circ\text{C}$ and $\Delta p_{\text{GaCl}} = 0.0016 \text{ atm}$, the molar flux is $N_{\text{GaAs}_{1-x}\text{P}_x} = 7.9 \times 10^{-9} \text{ gmoles/cm}^2\text{-sec}$. This corresponds to a linear growth rate of $0.77 \mu/\text{min}$.

LEGAL NOTICE

This report was prepared as an account of work sponsored by the United States Government. Neither the United States nor the United States Atomic Energy Commission, nor any of their employees, nor any of their contractors, subcontractors, or their employees, makes any warranty, express or implied, or assumes any legal liability or responsibility for the accuracy, completeness or usefulness of any information, apparatus, product or process disclosed, or represents that its use would not infringe privately owned rights.

TECHNICAL INFORMATION DIVISION
LAWRENCE BERKELEY LABORATORY
UNIVERSITY OF CALIFORNIA
BERKELEY, CALIFORNIA 94720